

INTEGRATED CLASSIFICATION AND ENHANCEMENT OF LOW LIGHT HAZY AND NOISY IMAGES

A DISSERTATION

Submitted in partial fulfillment of

the requirements for the award of the degree

of

MASTER OF TECHNOLOGY

in

ELECTRONICS AND COMMUNICATION ENGINEERING

(with specialization in Communication Systems)

By

ASHOK KUMAR SHEJWAL

(Enrollment No. 17531005)



DEPTT. OF ELECTRONICS AND COMMUNICATION ENGINEERING

INDIAN INSTITUTE OF TECHNOLOGY, ROORKEE,

ROORKEE-247667(INDIA)

JUNE 2019

CANDIDATE'S DECLARATION

I declare that the work presented in this dissertation with title “ **Integrated Classification and Enhancement of Low Light Hazy and Noisy Images**” towards the fulfillment of requirement for the award of degree of **Master of Technology** submitted in the **Department of Electronics and Communication Engineering, Indian Institute of Technology Roorkee**, India. It is an authentic record of my own work carried out under the supervision of **Dr. D Ghosh**, Professor, Department of Electronics and Communication Engineering, IIT Roorkee.

The content of this dissertation has not been submitted by me for the award of any other degree of this or any other institute.

DATE :

SIGNATURE:

PLACE: ROORKEE

(ASHOK KUMAR SHEJWAL)

CERTIFICATE

This is to certify that the statement made by the candidate is correct to the best of my knowledge and belief.

DATE :

SIGNATURE:

(DR. D GHOSH)

PROFESSOR
DEPT. OF ECE
IIT ROORKEE

Acknowledgment

On completion of my thesis, I am highly indebted to my guides Dr.D Ghosh (Professor, Department of Electronics and Communication Engineering) and Dr. M. J. Nigam (Retd.Professor, Department of Electronics and Communication Engineering) (currently, Professor JUIT Wakanghat) for constant guidance, support and motivation. During the dissertation period, they provided encouragement, good ideas, sound advice and lot of technical support. They always managed to spare time for my technical queries despite their busy schedule.

I would like to express my profound gratitude to my guides not only for their academic guidance but also for their interest in my dissertation work. Finally, I am extremely grateful to my Institution and batch-mates whose constant encouragement served to renew my spirit. I like to avail this opportunity to express a sense of respect and love to my friends and beloved family members for their strength and support.

(Ashok Kumar Shejwal)



Abbreviations

ANN	Artificial Neural Network
BM3D	Block Matching 3D
CDSA	Contrast Dependent Saturation Adjustment
CSL	Contrast Stretching Laplacian
DCP	Dark Channel Prior
FGF	Fast Guided Filter
HE	Histogram Equalization
LIME	Low light image enhancement via Illumination Map Estimation
LOE	Lightness Order Error
MLP	Multi Layer Perceptron
MOS	Mean Opinion Score
MSR	Multi Scale Retinex
MSE	Mean Square Error
NBPCPA	No Black Pixel constraints combined with Planar Assumption
NFERM	No reference Free Energy based Robust Metric
NIQE	Naturalness Image Quality Evaluator
NPEA	Naturalness Preserved Enhancement Algorithm
PI	Pixel Intensity
SSIM	Structure Similarity
SNR	Signal to Noise Ratio
SSR	Single Scale Retinex
SVM	Support Vector Machine
STD	Standard Deviation
VP	Visibility Parameter

Abstract

Images captured in low light environment losses out on details due to poor visibility conditions. These images are further degraded by noise and haze which result in contrast reduction, low visibility and color fading. The problem of haze removal is complicated since there is an inherent ambiguity between underlying scene and haze. Similarly, noise contained in an image may get amplified during haze removal. Hence, these unnecessary artifacts (haze and noise) are required to be removed before image enhancement in order to make non uniformly illuminated noisy and hazy images suitable for computer vision and multimedia based applications which are primarily designed for high-quality inputs.

This thesis proposes a novel integrated algorithm wherein image classification into Hazy, noisy and non-noisy is carried out automatically along with image enhancement. Since, the noise level in an image is not precisely known a priori, classification of image as noisy or non-noisy may lead to erroneous outcomes. Hence, image classification based on haze is carried out first. Hazy images are classified on the basis of visibility Parameter. Images with visibility parameter value lower than a threshold of 1.16 are treated as hazy and higher than 1.16 are treated as non-hazy. Non Hazy images are then tested for noise. Support Vector Machine classifier is used for classification of images into noisy and non-noisy category. After classification of images as hazy, noisy and non-noisy, different approaches are adopted for image enhancement. Multilayer Perceptron of Artificial Neural Network classes is used for haze removal. Noisy images are enhanced using Retinex based method which utilize image decomposition into reflectance and illumination component through iterative approach. Multi-Layer lightness statistics is used for enhancement of images which are neither hazy nor noisy.

A wide variety of low light noisy and hazy images are selected to evaluate the performance of proposed algorithm. Qualitative human evaluation with various state of the art and modern techniques of image enhancement is carried out, so that an assessment can be built for comparisons. Mean Opinion score is used for Qualitative evaluation. The results are further strengthen by Quantitative evaluation using various methods such as Lightness order error, Structure Similarity, Naturalness Image Quality Evaluator and No reference Free Energy based Robust Metric.

The method of image classification into hazy and noisy using visibility Parameter and Support Vector Machine Classifier is novel and works well for most of the images. The comparisons results presented in chapter 4 indicates that integrated approach has performed similar or better than other algorithms for enhancement of noisy and hazy images.

Contents

Acknowledgment	ii
Abbreviations	iii
Abstract	iv
List of Figures	viii
List of Tables	ix
Symbols and Notations	x
1 Introduction	1
1.1 Low Light Image processing	1
1.2 Motivation	1
1.3 Objectives	2
1.4 Outline of thesis	2
2 Literature Review	4
2.1 Hazy Image Enhancement	4
2.2 Noisy Image Enhancement	5
3 Low Light Image Classification and Enhancement	7
3.1 Visibility Parameter	7
3.2 Support Vector Machine Classifier	10
3.3 Image Dehazing	11
3.3.1 Multi-Layer Perceptron	11
3.3.2 MLP Training	12
3.3.3 Enhancement using DCP and MLP	13

3.4	Image Denoising	15
3.4.1	Reflectance Component	17
3.4.2	Illumination Component	17
3.4.3	Noise Component	17
3.4.4	Enhancement	18
3.5	Noiseless Image Enhancement	19
3.5.1	Image Decomposition	19
3.5.2	Multi-Layer Lightness Statistics	21
3.5.3	Image Enhancement	22
3.6	Metrics for Qualitative Analysis	24
3.6.1	Mean Opinion Score	24
3.6.2	Edge Detection	24
3.7	Metrics for Quantitative Analysis	24
3.7.1	Lightness Order Error	25
3.7.2	Structure Similarity	25
3.7.3	Naturalness Image Quality Evaluator	25
3.7.4	No reference Free Energy based Robust Metric	25
4	Results and Analysis	26
4.1	Qualitative Interpretation	26
4.1.1	Hazy Image Enhancement	26
4.1.2	Noisy Image Enhancement	32
4.1.3	Noiseless Image Enhancement	37
4.2	Qualitative Interpretation by Edge Detection for Noisy Image	42
4.3	Quantitative Measurement	43
4.3.1	Structure Similarity	43
4.3.2	Lightness Order Error	44
4.3.3	No reference Free Energy based Robust Metric	45
4.3.4	Naturalness Image Quality Evaluator	45
5	Conclusion and Future Work	46
	Bibliography	47

List of Figures

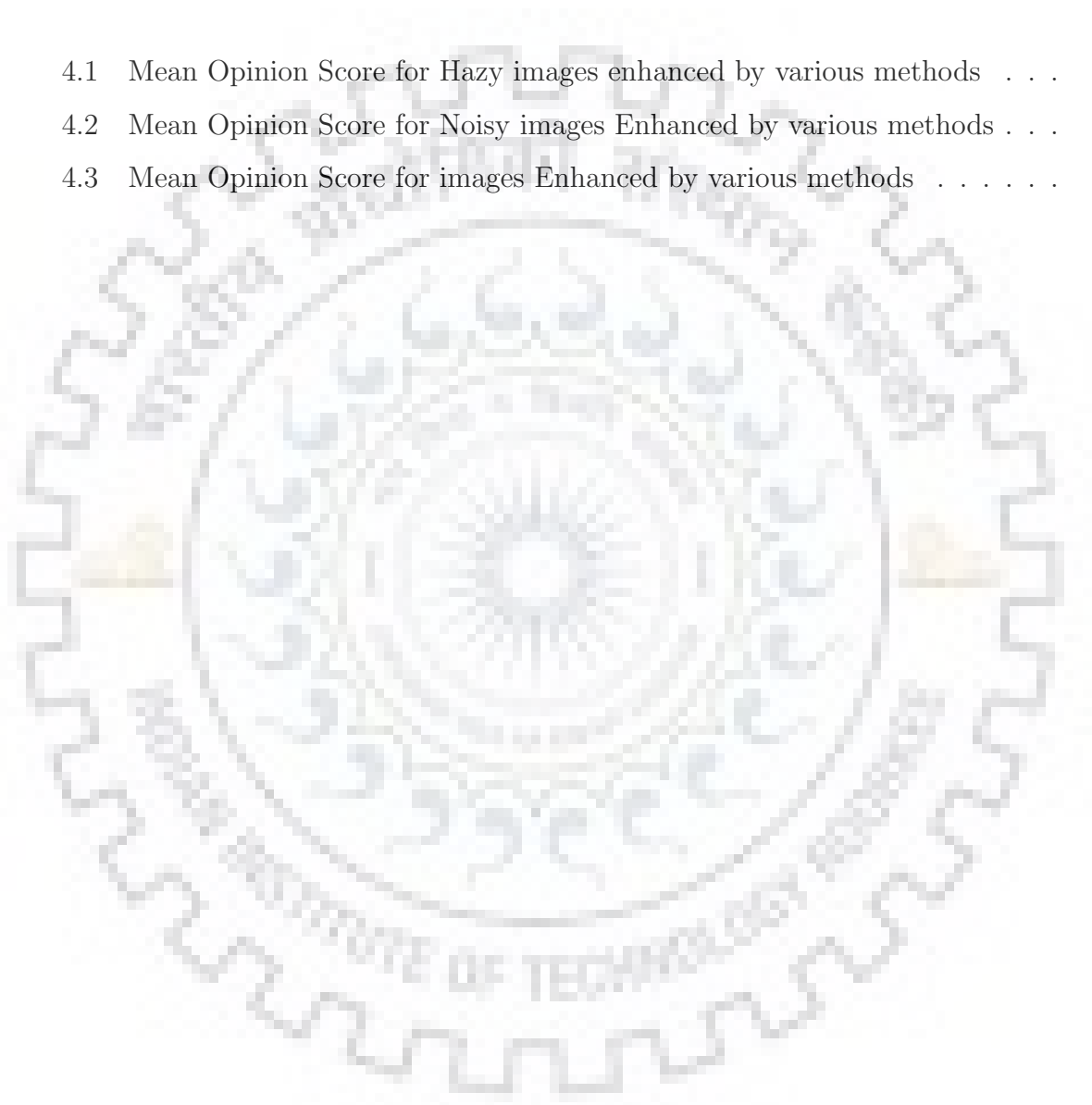
3.1	Flowchart of Image Classification and Enhancement Process	8
3.2	Hazy Images with Visibility Parameter Values	9
3.3	Non-Hazy Images with Visibility Parameter Values	10
3.4	Noisy Images Classified by SVM Classifier	11
3.5	Noiseless Images Classified by SVM Classifier	11
3.6	MLP Training Process	13
3.7	Hazy Image Enhancement	15
3.8	Components of Image	18
3.9	Noisy Image Enhancement	19
3.10	Image Decomposition	21
3.11	Average Lightness	22
3.12	Lightness Range	22
3.13	Image Decomposition and Enhancement flowchart	23
3.14	Noiseless Image Enhancement	23
4.1	Comparison of Hazy Image Enhancement by various methods	27
4.2	Comparison of Hazy Image Enhancement by various methods	28
4.3	Comparison of Hazy Image Enhancement by various methods	29
4.4	Comparison of Hazy Image Enhancement by various methods	30
4.5	Comparison of Noisy Image Enhancement by various methods	32
4.6	Comparison of Noisy Image Enhancement by various methods	33
4.7	Comparison of Noisy Image Enhancement by various methods	34
4.8	Comparison of Noisy Image Enhancement by various methods	35
4.9	Comparison of Noiseless Image Enhancement by various methods	37
4.10	Comparison of Noiseless Image Enhancement by various methods	38
4.11	Comparison of Noiseless Image Enhancement by various methods	39
4.12	Comparison of Noiseless Image Enhancement by various methods	40

4.13 Comparison of Sobel Edges in Noisy Image Enhanced by various methods	42
4.14 SSIM for Hazy Images	43
4.15 SSIM for Noisy Images	43
4.16 Average SSIM for Noiseless Images	44
4.17 LOE for Noiseless Images	44
4.18 NFERM for Noiseless Images	45
4.19 NIQE for Noisy Images	45

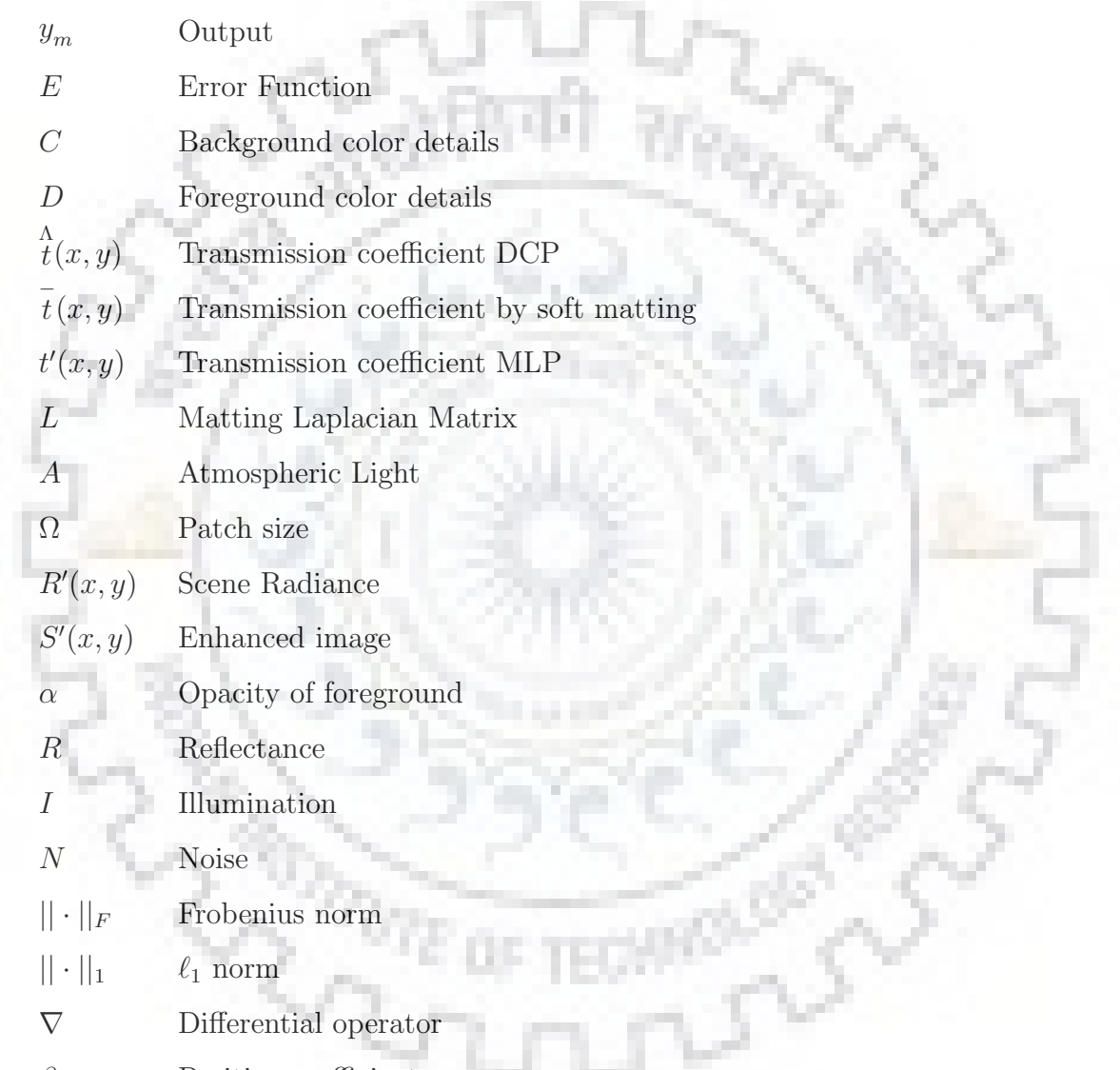


List of Tables

4.1	Mean Opinion Score for Hazy images enhanced by various methods . . .	31
4.2	Mean Opinion Score for Noisy images Enhanced by various methods . . .	36
4.3	Mean Opinion Score for images Enhanced by various methods	41



Symbols and Notations



$S(x, y)$	Input image
X_i	Multiple inputs
W_{ij}	Weights
b_j	Bias
\hat{y}_m	Desired output
y_m	Output
E	Error Function
C	Background color details
D	Foreground color details
$\hat{t}(x, y)$	Transmission coefficient DCP
$\bar{t}(x, y)$	Transmission coefficient by soft matting
$t'(x, y)$	Transmission coefficient MLP
L	Matting Laplacian Matrix
A	Atmospheric Light
Ω	Patch size
$R'(x, y)$	Scene Radiance
$S'(x, y)$	Enhanced image
α	Opacity of foreground
R	Reflectance
I	Illumination
N	Noise
$\ \cdot\ _F$	Frobenius norm
$\ \cdot\ _1$	ℓ_1 norm
∇	Differential operator
β, ω	Positive coefficients
G	Guidance Matrix

λ, σ	Controls degree of amplification and rate
γ	Gamma correction
k	Iteration
μ, δ	Positive scalar
Z	Lagrange's Multiplier
$I_i(x, y)$	Low-frequency component
$R_i(x, y)$	High-frequency component
$I_n(x, y)$	Low-frequency component of the last layer
$R_c(x, y)$	High-frequency component by decomposing input image
$\overline{I(i)}$	Average lightness
$\overline{R(i)}$	Lightness range
$W(x, y)$	Normalizing factor
R_n	Individual ratings on a stimulus by N subjects
\oplus	Exclusive or operator



Chapter 1

Introduction

1.1 Low Light Image processing

Application of computer algorithms to digital images for processing is known as Digital Image Processing. It is a part of signals and systems which focus particularly on images. A high visibility image contains lot of visual information such as scene's object, color, brightness, background etc. These information's are critical for computer vision based techniques such as object detection, tracking, remote sensing, surveillance etc. But, images cannot be captured in high visibility condition always. Images captured in low light conditions often suffer from poor visibility. This is further complicated by noise (due to sensor error of cameras), haze and other atmospheric degradation. Image enhancement techniques for low light images degraded by noise, haze, smog, rain etc. is an active research area wherein good amount of research has been carried out and still researchers are trying for better and sophisticated algorithm to achieve better performance.

1.2 Motivation

Image enhancement initially stated with Retinex theory wherein an uniformly illuminated image is decomposed into two components: illumination and reflectance. Illumination components is normally ignored and reflectance components is treated as enhanced image. New techniques and method for low light image enhancement were built which keep both illumination and reflectance components during image enhancement as low light images are not uniformly illuminated. Techniques were further developed for low light noisy and hazy images wherein both types of degradation are normally treated separately. While

carrying out literature survey, a need was felt to develop an integrated approach for image enhancement of low light and noisy image wherein image are automatically segregated as hazy, noisy or non-noisy and appropriate methods can be utilized after image classification for enhancement based on the type of degradation. Hence, the motivation to study and propose a technique which can cater for above requirement got conceived and this thesis is presenting proposed approach with all possibilities.

1.3 Objectives

- The primary objective is to propose an algorithm which can take an image as an input, classify the image as hazy or non-hazy based on visibility value of each image. Hazy images have low visibility in comparison to non-hazy image. If image is non hazy, a suitable Classifier to be identified for classification of image as noisy and non-noisy.
- After image classification, suitable methods to be proposed through algorithm which can cater for enhancement of hazy, noisy and non-noisy images.
- Next objective is to carry out qualitative result analysis of the enhanced images for naturalness, sharpness, edge continuity, haze and noise removal. The comparison should not be only on quantitative basis. The results obtained by proposed method shall be compared with state of art and modern techniques of noise and haze removal in order to assess the quality of results.
- In order to make the comparison ideal, wide variety of images shall comply with different lighting conditions, background and textures, with different haze condition (low, medium and thick) and natural noise. The comparison results have to be developed not for two or three images but at least for 30-40 images variety.

1.4 Outline of thesis

The thesis is organized as follows:

- Chapter 2 gives the literature survey carried out for the thesis for which an extensive study has been carried out of the existing research in field of low light noisy and hazy image enhancement.

- Chapter 3 covers introduction to visibility parameter and Support vector Machine (SVM) used for classification of hazy and Noisy images respectively. Further different methods for enhancement of low light hazy, noisy and non-noisy images are explained. A detailed flowchart depicting the complete procedure followed in retrieving enhanced low light images has been presented.
- Results and Analysis on variety of images with inferences drawn are presented in Chapter 4.
- Conclusion with future scope is drawn in chapter 5.



Chapter 2

Literature Review

High visibility images provides clear details (like object, background, contrast, color, edges etc.) of the target scenes. These details are critical for many vision based method utilized in surveillance, remote sensing, traffic control, weapon engagement and autonomous driving applications [1] [2]. But, these details are lost in low visibility images. These images are further degraded by addition of atmospheric conditions of haze, dust, rain etc. and sensor noise. The atmospheric degradation and sensor noise is removed in low light images by various image enhancement methods. The image enhancement methods normally deals with only a single type of degradation.

2.1 Hazy Image Enhancement

Haze is an atmospheric phenomenon in which turbid media diminishes the details reflected by the scene. A low light hazy image can be low, medium or high haze. Ramesh *et.al* [3] proposed equation for classification of color hazy images.

The issue of Haze removal is widely studied. The strategies used for haze removal can be classified based on input information such as multiple target [4] [5], three-dimensional data [6] and use of single image [7]. The single image based approach is most studied due to non-availability of additional data [8]. For single image dehazing, Tarel *et.al* [9] proposed two different filters: a filter for preserving edges and corners and a median filter. Haze removal from an image is based on estimates of scattered air light. He *et.al* [10] proposed the Dark Channel Prior (DCP) algorithm which is a statistical analysis of images without haze. It is used to compute the transmission and restore back the image using atmospheric scattering model. DCP algorithm gives good results in most of the

cases. The major drawback of DCP is its intensive computational processing required to refine a generated coarse transmission, which makes it unsuitable for applications where response time is small. Further improvements to DCP were proposed. Pang *et.al* [11] proposed to dehaze the image using edge preserving smoothing operator named as guided filter having a patch radius of 30.

Artificial neural network (ANN) have started to garner attention in computer vision application. ANN are computing systems based on biological neural network which tries to emulate the micro structure of the brain. Multilayer Perceptron (MLP) [12] is the most popular ANN classes because of its ease of application and robustness. MLP has at least three layers of neurons which uses a supervised learning strategy known as back-propagation [13]. MLP is used to solve denoising, facial recognition, skin segmentation and dehazing problems of image processing [14].

2.2 Noisy Image Enhancement

Low light images has often inherent noise caused by the hardware. This noise can be addressed by increasing the exposure time of image capturing device. Higher exposure time increases Signal to Noise Ratio (SNR) and generates noise-free image but, a higher exposure time may lead to blur. Thus classification of image as noisy or noise free is a challenging task. Classification of noisy and noise free images can be carried out based on classifiers. Binary Support Vector Machine (SVM) [15] based classifier classifies the input image as noisy or noise free.

The low light images have low SNRs which makes its enhancement as a non trivial activity. Noises in captured scene are intensive which may dominate over important image signals. Hence, low light image enhancement algorithms should be able to handle low light and high level noises, along with poor contrast. Low light images can be enhanced by amplifying the illumination directly. But, this may result in saturation of bright area and loss of details.

Methods [16] [17] which uses Histogram Equalization (HE) stretches the dynamic range of the input images to reduce the problem to a level. But, these methods results in images which are either over or under enhanced. Retinex theory [18] studied extensively in past assumes that image lightness consists of two components i.e., illumination (amount of radiant flux received by scene) and reflectance (capability to reflect the radiant energy).

The reflectance components has correlation to various color sensations and hence emerged as primary components for initial retinex-based methods such as SSR [19] and MSR [20] which enhances an image through removal of estimated illumination components. The results obtained by these methods often looks unnatural. Even though logarithmic transformation is widely used in retinex based methods, it is not appropriate for regularization the terms since, variation terms which are in the high magnitude area are dominated by low magnitude pixels. Due to significance of illumination component in enhanced image, many recent methods [21] [22] resort to compression of illumination component rather than removal of it completely. A bright pass filter was proposed by Wang *et.al* [23] for decomposition of observed image into illumination and reflectance. It preserves naturalness of the image while enhancing the details. In order to enhance an observed image naturally, a priori statistics of natural scenes is helpful. Wang *et.al* [24] proposed a multi-layer lightness statistics based image enhancement techniques which carries out natural enhancement of low light images. Even though these methods enhances non-noisy images well, results for noisy images is not so promising since constraints for reflectance are not well defined. Also, intensive noise component present in the image is increased rather than reducing.

In order to address the issue of intensive noise, a joint bilateral filter [25] is used to suppress the intensive noise. Li *et.al* [26] enhances the visual quality of observed image by segmenting it into superpixels and then utilizing BM3D [27] adaptively on different segments. The results obtained are reasonable but sequencing of image denoising or enhancing is a trivial issue. Noise gets amplified if image is enhanced before denoising whereas, image enhancement after denoising may result in blurred image. Mading li *et.al* [28] proposed retinex based method wherein additional noise term is added for the intensive noise term.

In this thesis, integrated approach for classification of low light imageries into hazy, noisy and non-noisy is exploited. The classified low light imageries are then enhanced using different techniques such as Multilayer Perceptron for haze removal [14] and retinex based approaches [24] [28] for enhancement of noisy and non-noisy images.

Chapter 3

Low Light Image Classification and Enhancement

Image enhancement is the core area of research and advancement in order to maintain the inherent details and naturalness of low light images. It makes the input image more useful for display and analysis by accentuation or sharpening its features such as contrast, edges and boundaries. The inherent information content provided by the input data should not increase after the enhancement process.

In order to enhance low light images, the removal of inherent haze and noise from the image is an important aspect. Before removal of haze and noise, it is important to classify images into various categories (hazy, noisy, non-noisy etc.) in order to apply appropriate method for removal of artifact and enhancement. The segregation of image as hazy or non-hazy can be carried out using Visibility parameter. The flow chart depicting the complete process of classification and Enhancement is given in Fig. 3.1.

3.1 Visibility Parameter

The amount of atmospheric light reflected from a Hazy image(S) is greatly dependent on the amount of haze present in the image. A dense hazy image reflects less light in comparison to thin hazy image. The image parameters such as mean(m), Standard Deviation(STD) are affected by the amount of haze present in an image. The Equation for Visibility Parameter(VP) based on these two image parameters and Pixel Intensity(PI) is given by:

$$VP = \frac{\sqrt{STD} * PI^2}{m} \quad (3.1)$$

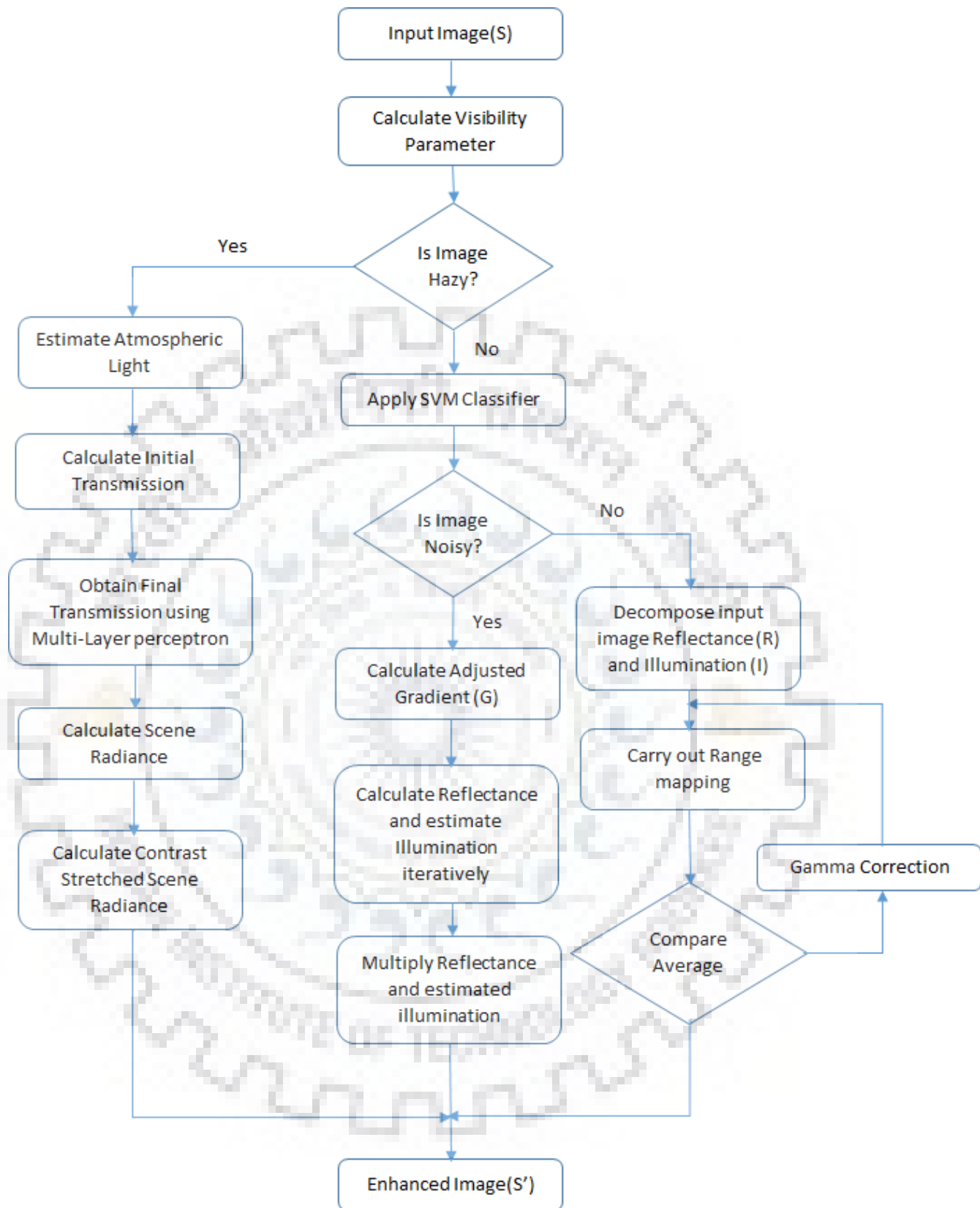


Fig. 3.1. Flowchart of Image Classification and Enhancement Process

wherein,

$$m = \frac{1}{MN} \sum_{x=0}^{M-1} \sum_{y=0}^{N-1} s(x, y) \quad (3.2)$$

$$STD = \sqrt{\frac{1}{MN} \sum_{x=0}^{M-1} \sum_{y=0}^{N-1} (s(x, y) - m)^2} \quad (3.3)$$

$$PixelIntensity(PI) = \maxintensity - \minintensity \quad (3.4)$$

M,N -size of image.

The Visibility parameter threshold is determined as 1.16 by evaluating it on more than 150 images. The images with a visibility parameter less than 1.16 is hazy and higher than 1.16 is non-hazy. This leads to classification of images as hazy or non-hazy with an accuracy of 95% . The method to enhance hazy images is given in section 3.3. Dehazing of images is carried out before denoising. This avoids increase of latent error which might increase due to “under-denoising” or “over denoising” if carried out before dehazing.



(a) 1.1524



(b) 0.9105



(c) 0.8736



(d) 0.139

Fig. 3.2. Hazy Images with Visibility Parameter Values

In the Fig. 3.2, (a) has the highest visibility parameter value whereas (d) has the least. The visibility parameter value for Non-Hazy is shown below in Fig. 3.3. The haze deteriorate visibility of an image can be observed from above results.



(a) 2.3446



(b) 2.4400



(c) 1.7678



(d) 1.5008

Fig. 3.3. Non-Hazy Images with Visibility Parameter Values

3.2 Support Vector Machine Classifier

The non-hazy images are further classified as noisy or non-noisy. For this, a binary SVM classifier is used. It builds a model so that classes for new test images can be identified. The new images were fit into one of these classes.

The parameters used for training of SVM classifiers is based on Haralick Texture Features [29]. 14 parameters are used in training of SVM classifier. The Parameters includes Angular second moment, Information Measure of correlation, Contrast, Correlation, Maximal correlation coefficient, Variance, Sum Average, Entropy etc. All these parameters extract important details of each image which helps in creating benchmark for separation of input images into various categories. 70 Noisy and 70 Noiseless natural images are taken for training of classifier. After training of SVM classifier, images are tested and classified as noisy or noiseless with an accuracy of 85% .



Fig. 3.4. Noisy Images Classified by SVM Classifier

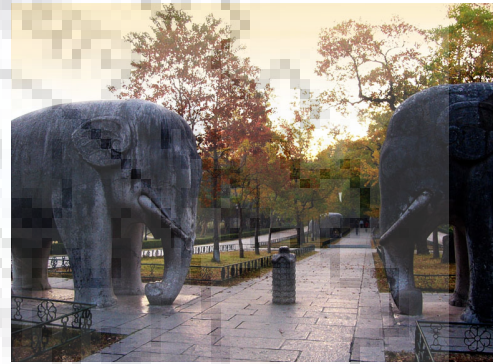


Fig. 3.5. Noiseless Images Classified by SVM Classifier

After classification of the images into various categories, next step is to enhance the images. Single type of image degradation is only resolved i.e., either haze or noise is removed.

3.3 Image Dehazing

The problem of haze reduction or elimination is necessary in image processing. The Removal of Haze can be carried out using Artificial Neural Network(ANN). One such class of ANN used here for image enhancement is Multi-Layer Perceptron(MLP).

3.3.1 Multi-Layer Perceptron

The Perceptron is a processing element (called as neurons) which has multiple inputs. It has three layers namely, input, intermediate(hidden) and output. The connections between processing elements which are present in one or more hidden layers forms a

network. The processing element [14] is given by:

$$Y_j = f\left[\sum_i (W_{ij} * X_i + b_j)\right] \quad (3.5)$$

wherein,

X_i - Multiple inputs

W_{ij} - Weights

b_j - Bias

Hyperbolic tangent function is used as activation function (f) in Perceptron which is expressed as:

$$\tanh(x) = 2 \bullet \sigma(2x) - 1 \quad (3.6)$$

wherein,

$$\sigma(x) = \frac{e^x}{1 + e^x} \quad (3.7)$$

To obtain the desired output, weight and bias values are adjusted during the training of ANN according to the input combinations. MLP is trained through back-propagation which is generalization of least square method wherein Mean Square Error (MSE) for weight updation is given by:

$$E = \frac{1}{2} \sum_{j \in M} (\hat{y}_m - y_m) \quad (3.8)$$

wherein,

\hat{y}_m being the desired output for the y_m .

3.3.2 MLP Training

The ground truth data for MLP [14] is computed using the soft mating algorithm [30]. The soft mating of image can be carried out as

$$S = C\alpha + D(1 - \alpha) \quad (3.9)$$

wherein, C and D represents background and foreground color details respectively. The opacity of foreground is represented by α .

Since α map and transmission map are equivalent, optimal $\bar{t}(x, y)$ can be computed by

$$(L + \lambda U) \bar{t} = \lambda \hat{t} \quad (3.10)$$

wherein,

$\lambda = 10^{-4}$

\hat{t} - transmission computed through Dark Channel Prior(DCP)

L - Matting Laplacian matrix

U - Identity matrix of size as L

In order to train MLP, 74 test images are taken which are trained using eq. 3.11 and applying soft matting method to $t_{\min}(x, y)$. Two vectors of samples: input and target vectors are required for MLP training. The samples are acquired by a square window of size M centered at (x, y) . The length for each sample is $M \times M$. $t_{\min}(x, y)$ and $\hat{t}(x, y)$ is used to obtain input and target vector respectively. The sampling interval $\beta = 8$ and window size $s = 16$. The training process for MLP is shown in Fig. 3.6.

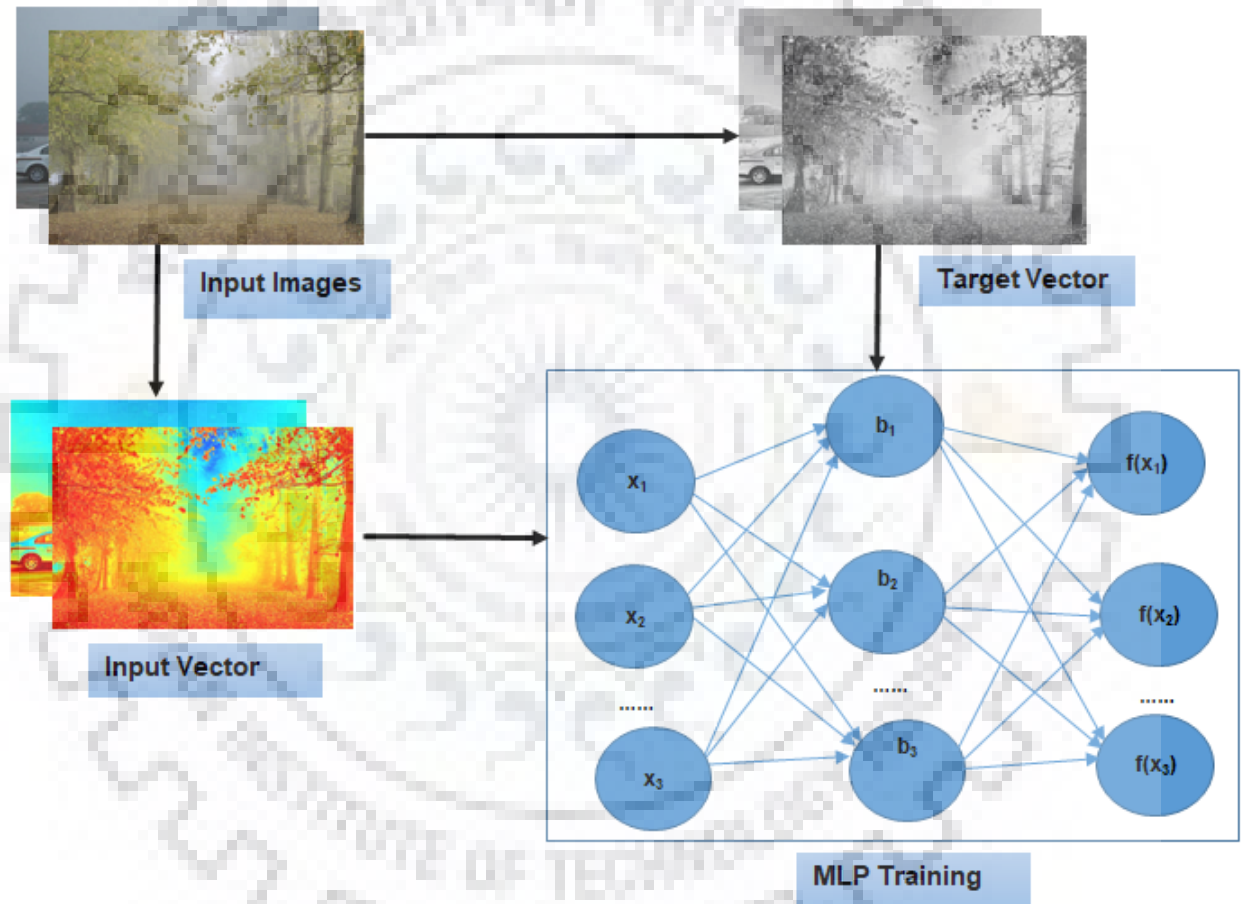


Fig. 3.6. MLP Training Process

3.3.3 Enhancement using DCP and MLP

The DCP [10] based image dehazing methods have two stages for transmission map estimation. Firstly, a coarse transmission map is estimated based on square patches of predefined size. Secondly, the coarse transmission map is modified by different filtering strategies such as bilateral, median, guided etc.

The trade-off between computational time and accurate restoration is the main disadvantage of these strategies. In MLP based method, the transmission map $t_{\min}(x, y)$ [14] is defined as

$$t_{\min}(x, y) = 1 - \omega S^{\min}(x, y) \quad (3.11)$$

wherein,

$$S^{\min}(x, y) = \min_{c \in (R, G, B)} \frac{S^c(x, y)}{A^c} \quad (3.12)$$

Atmospheric light is defined as

$$A^c = \max \sum_{c=1}^3 S^c \left\{ \max_{\Omega \in (0.001 * h * w)} [S^{dark}(x, y)] \right\} \quad (3.13)$$

wherein,

Ω - patch size

$h * w$ - height and width of $S^{dark}(x, y)$

c-R,G,B channels of $S(x, y)$

The depth resolution of $t_{\min}(x, y)$ is low due to omission of details of neighboring pixels.

Therefore, ANN MLP is used to estimate transmission map $t'(x, y)$ [14] given by

$$t'(x, y) = MLP[t_{\min}(x, y)] \quad (3.14)$$

In order to obtain image without affectations, $R'(x, y)$ (scene radiance) [14] is given by

$$R'(x, y) = \frac{S(x, y) - A}{t'(x, y)} + A \quad (3.15)$$

In the proposed method, $L * a * b$ space color and a contrast stretching strategy [31] is used to estimate transmission map and to improve the contrast of the recovered image.

The final dehazed image is given by:

$$S'(x, y) = CSL[R'(x, y)] \quad (3.16)$$

The dehazed images are presented in Fig. 3.7.



(a) *InputImage*

(b) *EnhancedImage*

Fig. 3.7. Hazy Image Enhancement

3.4 Image Denoising

An image can be decomposed into reflectance and illumination components as proposed by Classical Retinex theory [18]. Image can be defined as:

$$S = R \circ I, \quad (3.17)$$

wherein,

S - input image,

R - Reflectance component,

I - Illumination component,

\circ - element-wise multiplication.

The classical models based on retinex does not considered the inherent noise term N which exist in the low light imageries, hence are not suitable for them. Hence, a modified model to entertain the noise should be built as:

$$S = R \circ I + N. \quad (3.18)$$

The illumination component I is emphasized in most methods to obtain reflectance R

which is given as $R = S/I$, wherein, the noise component N is neglected. This results in reflectance image as $R' = R + N/I$ which has an unpleasant noise in it.

Due to these reasons, reflectance R and illumination I are optimized iteratively taking noise as one of the factor affecting them. The decomposition equation [28] is given by:

$$\min_{R,I,N} \|R \circ I + N - S\|_F^2 + \beta \|\nabla I\|_1^2 + \omega \|\nabla R - G\|_F^2 + \delta \|N\|_F^2 \quad (3.19)$$

$\|\cdot\|_F$ represents Frobenius norm and $\|\cdot\|_1$ is the ℓ_1 norm respectively. The first order differential operator is ∇ . β and ω are positive coefficients for controlling importance of terms in the equation. The role of each term is interpreted below:

$\|R \circ I + N - S\|_F^2$ - fidelity constraints between recomposed image $R \circ I$ and observed image S in presence of noise N ,

$\beta \|\nabla I\|_1^2$ -represents the total variational sparsity and consider piecewise smoothness of illumination map I ,

$\omega \|\nabla R - G\|_F^2$ -reduces the gap between gradient of reflectance R and guidance matrix G of the observed image S in order to strengthen the contrast of final result,

$\delta \|N\|_F^2$ -represents overall intensity of noise.

Enhancing the gradient of input image by a factor P , the guidance matrix G can be obtained. The small gradient (i.e., noise) is suppressed before amplification. The factor P is designed to balance magnitude of G in such a way that it makes higher adjustments in areas of lower magnitudes and vice versa. The G can be formulated as:

$$G = P \circ \nabla \hat{S} \quad (3.20)$$

$$P = 1 + \lambda e^{-|\nabla \hat{S}|/\sigma} \quad (3.21)$$

$$|\nabla \hat{S}| = \begin{cases} 0, & \text{if } |\nabla S| < \varepsilon \\ \nabla S, & \text{otherwise} \end{cases} \quad (3.22)$$

Where, λ and σ controls degree and rate of amplification for various gradients respectively. To make the equation simpler, we replace ∇I by V . Equation 3.19 changes to

$$\min_{R,I,N} \|R \circ I + N - S\|_F^2 + \beta \|V\|_1^2 + \omega \|\nabla R - G\|_F^2 + \delta \|N\|_F^2 \quad (3.23)$$

To remove the equality constraint, Lagrange multiplier Z is introduced. Equation 3.23 changes to

$$\min_{R,I,N,T,Z} \|R \circ I + N - S\|_F^2 + \beta \|V\|_1^2 + \omega \|\nabla R - G\|_F^2 + \delta \|N\|_F^2 + \phi(Z, \nabla I - V) \quad (3.24)$$

3.4.1 Reflectance Component

To obtain the reflectance component of the observed image, we neglect the terms which are not related to R . Equation 3.24 reduces to

$$\min_R \|R \circ I + N - S\|_F^2 + \omega \|\nabla R - G\|_F^2 \quad (3.25)$$

The first term of the above equation can be reformulated to make it a least square problem given by:

$$\min_R \|\bar{i}^k r + n^k - s\|_F^2 + \omega \|\nabla R - G\|_F^2 \quad (3.26)$$

where i is vectorized form of I , \bar{i} has i as the entries in diagonal matrix form. Same notation is used for other parameters. k indicates the iteration. Differentiating with R and equating it to 0, we get

$$2(\bar{i}^k)^T(\bar{i}^k r + n^k - s) + 2\omega D^T(Dr - g) = 0 \quad (3.27)$$

$$((\bar{i}^k)^T \bar{i}^k + \omega D^T D)r = (\bar{i}^k)^T(i - n^k) + \omega D^T g \quad (3.28)$$

$$r^{k+1} = ((\bar{i}^k)^T(i - n^k) + \omega D^T g) / ((\bar{i}^k)^T \bar{i}^k + \omega D^T D) \quad (3.29)$$

3.4.2 Illumination Component

For the illumination component, we ignore the terms which are not related to I . Equation 3.24 reduces to

$$\min_I \|R \circ I + N - S\|_F^2 + \beta \|\nabla I\|_1^2 \quad (3.30)$$

Similar to reflectance, the solution for I can be written as

$$i^{k+1} = (2\bar{r}^{k+1}(s - n^{k+1}) + \mu D^T(t^k - z^k/\mu)) / (2((\bar{i}^{k+1})^T \bar{i}^{k+1} + \mu D^T D)) \quad (3.31)$$

3.4.3 Noise Component

The noise component can be obtained by neglecting terms other than N . Equation 3.24 reduces to

$$\min_N \|R \circ I + N - S\|_F^2 + \delta \|N\|_F^2 \quad (3.32)$$

The solution for N can be obtained as

$$N^{k+1} = (S - R^{k+1} \circ I^{k+1}) / (1 + \delta) \quad (3.33)$$

wherein, division is performed element wise. Similarly, the parameters V , Z and μ can be solved and written as

$$T^{k+1} = F_{\beta/\mu^k}(\nabla I^{k+1} + (Z^k/\mu^k)) \quad (3.34)$$

wherein, F represents shrinkage operation. It is defined as

$$F_\varepsilon(x) = \text{sign}(x) \max(|x| - \varepsilon, 0) \quad (3.35)$$

Calculation are carried out element-wise in above eq. 3.35.

$$Z^{k+1} = Z^k + \mu^k(\nabla I^{k+1} - V^{k+1}) \quad (3.36)$$

$$\mu^{k+1} = \mu^k \rho \quad (3.37)$$

The process stops if the difference between two successive iteration is 10^{-4} . The initial parameters for the iterations is given by $I^0 = S, N^0 = Z^0 = T^0 = k = 0, \mu = 1, \rho = 1.5$. The value for δ and ε is 9 & 0.039 respectively. The various components of the image are shown in Fig. 3.8.

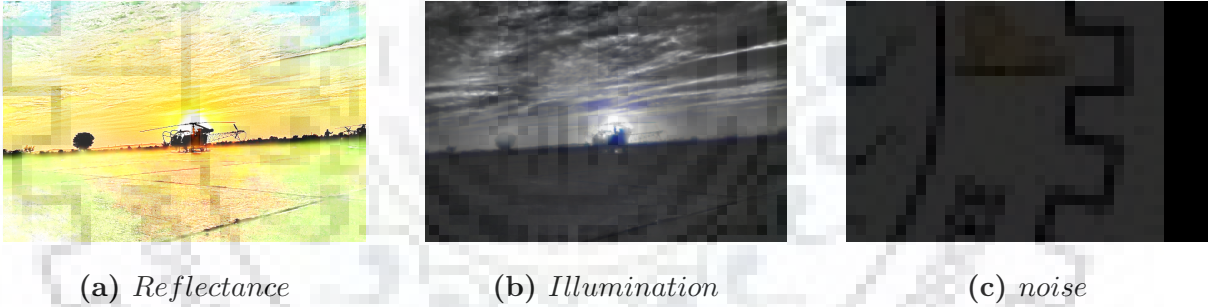


Fig. 3.8. Components of Image

3.4.4 Enhancement

Gamma correction is applied to adjust the illumination I' , once the illumination I and reflectance components R are estimated. The enhanced output image S' is given by

$$S' = R \circ I'^\gamma \quad (3.38)$$

wherein γ is set to 2.2 empirically. The enhanced noisy images are shown in Fig. 3.9.



Fig. 3.9. Noisy Image Enhancement

3.5 Noiseless Image Enhancement

The noiseless low light images often suffer from unnatural enhancement. The enhancement of low light images keeping naturalness intact can be carried out using multi-layer lightness statistics model [24] designed a priori using high quality outdoor images. The enhancement of images is carried out as explained below:

1. Using a multi-layer model to extract details of low frequency components layer by layer successively.
2. To enhance low-frequency component of low light images by using prior derived multi-layer lightness from high-quality outdoor images.
3. Overall image quality assessment for contrast enhancement and naturalness preservation.

3.5.1 Image Decomposition

Each illumination component $I_i(x, y)$ of input image can be decomposed into a illumination component $I_{i+1}(x, y)$ and a reflectance component $R_{i+1}(x, y)$ using a low-pass filter (Associative Filter [32]).

The high frequency Component is given by

$$R_{i+1}(x, y) = \frac{(I_i(x, y))}{(I_{i+1}(x, y))} \quad (3.39)$$

The lightness range shrinks as i increase for the low frequency component. The lightness will be uniform of last layer $I_n(x, y)$ if layer number i is large. Each $R_i(x, y)$ has some frequency details of input image, which are combined in order to preserve the details in the final enhanced image. The expression for image decomposition [24] can be given by

$$S^c(x, y) = R^c(x, y) \prod_{i=1}^n R_i(x, y) \bullet I_n(x, y) \quad (3.40)$$

where,

$I_i(x, y)$ - Illumination component,

$R_i(x, y)$ - Reflectance component,

$I_n(x, y)$ -Illumination component of last term, and

$R_c(x, y)$ -Reflectance term by decomposing the input image $S^c(x, y)$ directly.

Associative Filter

The Decomposition of image is achieved through an associative filter [32]. It is defined as

$$I_{i+1}(x, y) = \frac{1}{w(x, y)} \sum_{(x', y') \in \Omega(x, y)} \left(\exp\left(\frac{-(I_i^{cs}(x', y') - I_i(x, y))^2}{2\sigma^2}\right) \right) \quad (3.41)$$

wherein,

$i=0, 1, 2, 3, \dots, n-1$

$\Omega(x, y)$ - 31X31 patch at (x, y) ,

$\sigma = 3$,

$I_i^{cs}(x, y)$ -local maxima of $I_i(x, y)$.

$I_i^{cs}(x, y)$ is given by

$$I_i^{cs}(x, y) = \max_{(\hat{x}, \hat{y}) \in \Omega'(x, y)} I_i(\hat{x}, \hat{y}) \quad (3.42)$$

wherein,

$\Omega'(x, y)$ -15X15 patch at (x, y) ,

The normalizing factor $W(x, y)$ is defined as

$$W(x, y) = \sum_{(x', y') \in \Omega(x, y)} \left(\exp\left(\frac{-(I_i^{cs}(x', y') - I_i(x, y))^2}{2\sigma^2}\right) \right) \quad (3.43)$$

The decomposition of an image is complete when there no variation in the low frequency components as shown in Fig. 3.10.

3.5.2 Multi-Layer Lightness Statistics

The associative filter is used for decomposition of image into multiple layers. The maximum limit on number of layer is 26, since, the details in illumination terms of decomposed images is uniform in 26 iterations.

The average lightness $\overline{I(i)}$ [24] and lightness range $\overline{R(i)}$ [24], for decomposed images can be calculated as:

$$\overline{I(i)} = \frac{1}{N} \sum_{p=1}^N I_p(i) , i = 0, 1, 2, \dots, 25 \quad (3.44)$$

$$\overline{R(i)} = \frac{1}{N} \sum_{p=1}^N R_p(i) , i = 0, 1, 2, \dots, 25 \quad (3.45)$$

wherein,

N - decomposed image number,

$I_p(i) = \text{mean } I_i(x, y)$ i.e., average lightness of the illumination component $I_i(x, y)$ of image p,

$R_p(i) = \max I_i(x, y) - \min I_i(x, y)$ gives the lightness range of decomposed images.



Fig. 3.10. Image Decomposition

The plot of Average lightness in Fig. 3.11 demonstrates that the Average illumination increases with increase in layer index as more details are added with successive layers. The lightness range plot in Fig. 3.12, demonstrates that illumination range decreases with increase of layer index i , since, details are extracted in successive layers.

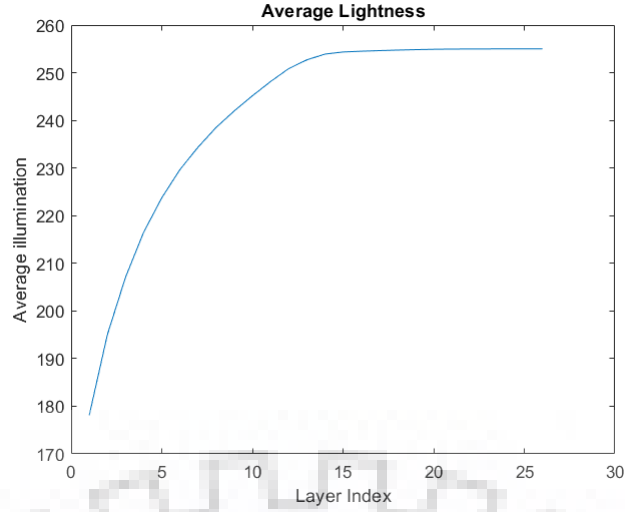


Fig. 3.11. Average Lightness

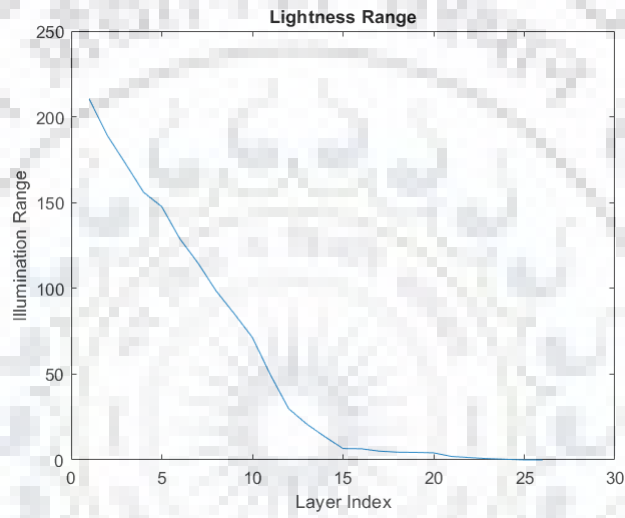


Fig. 3.12. Lightness Range

3.5.3 Image Enhancement

After lightness statistics is built up, low frequency components are enhanced using mapping. The modification is carried out as follows:

$$g(I_i(x, y)) = \frac{G_i(x, y) - \min(G_i(x, y))}{\max(G_i(x, y)) - \min(G_i(x, y))} \bullet \overline{R(i)} + (255 - \overline{R(i)}) \quad (3.46)$$

$$G_i(x, y) = (I_i(x, y))^\gamma \quad (3.47)$$

wherein,

$I_i(x, y)$ - interval of $[255 - \overline{R(i)}, 255]$

γ - to tune the low frequency to satisfy eq. 3.44. Once, all the low frequency components are mapped, the image can be finally enhanced as shown by eq. 3.48 and flow chart Fig 3.13.

$$S_e^c(x, y) = R^c(x, y) \cdot \prod_{i=0}^{n-1} \left(\frac{g(I_i(x, y))}{g(I_{i+1}(x, y))} \right) \cdot g(I_n(x, y)) \quad (3.48)$$

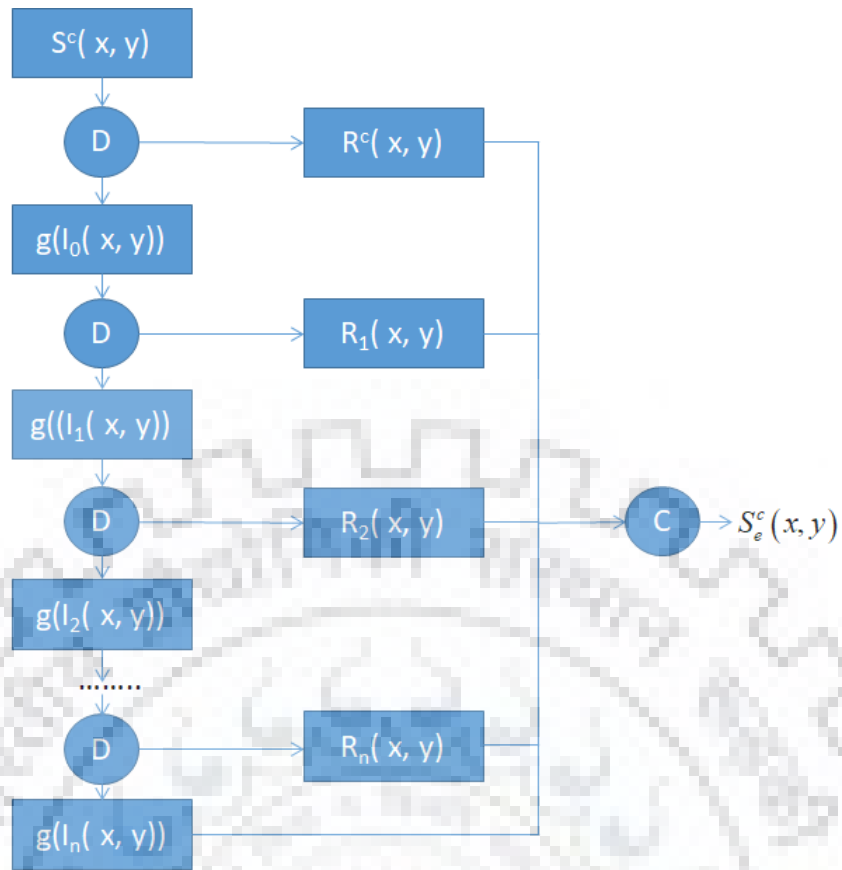


Fig. 3.13. Image Decomposition and Enhancement flowchart

The Enhanced image are shown in Fig. 3.14.



Fig. 3.14. Noiseless Image Enhancement

3.6 Metrics for Qualitative Analysis

To carry out qualitative analysis of proposed algorithm with other techniques, Mean Opinion Score(MOS) [33] and edge detection tool is used. Brief of these methods is provided below.

3.6.1 Mean Opinion Score

The Mean Opinion Score is a single rational number in the range of 1–5, where 1 and 5 is the lowest and highest perceived quality respectively.

MOS is given by:

$$MOS = \frac{\sum_{n=1}^N R_n}{N} \quad (3.49)$$

wherein, R defines the individual ratings by N subjects on a given stimulus.

Higher the mean opinion score, better the enhanced image.

3.6.2 Edge Detection

A high quality enhanced image preserves edges better than non enhanced image. If input image has noise, a better enhanced image will have less noise with details well preserved. There are various method for edge detection such as sobel, prewitt, canny, susan etc. [2] [1] which can be tried on enhanced image for qualitative interpretation.

3.7 Metrics for Quantitative Analysis

To carry out quantitative analysis of proposed algorithm with other techniques for noise, haze and noiseless image enhancement, famous and time tested metrics like Lightness Order Error [23], Structure similarity [34], Naturalness Image Quality Evaluator [35] and No reference Free Energy based Robust Metric [36]. These methods gives out values based on the mathematics involved when applied to the input and enhanced image. The results obtained are plotted on graph for interpretation and decision making in order to evaluate performance of different enhancement techniques. Succeeding paragraph provide details of evaluation metrics in brief.

3.7.1 Lightness Order Error

The LOE [23] measure is used for determination of lightness inequality preservation. Its value indicates average number of pixel pairs for which, lightness inequality after enhancement is reversed. LOE is defined as:

$$LOE = \frac{1}{m \bullet n} \sum_{i=1}^m \sum_{j=1}^n RD(i, j), \quad (3.50)$$

$$RD(i, j) = \sum_{i=1}^m \sum_{j=1}^n (U(I(x, y), I(i, j)) \oplus U(I_e(x, y), I_e(i, j))), \quad (3.51)$$

$$U(x, y) = \begin{cases} 1, & \text{for } x \geq y \\ 0, & \text{else} \end{cases} \quad (3.52)$$

wherein,

$I(i, j)$ - pixel lightness before enhancement,

$I_e(x, y)$ - pixel lightness after enhancement,

m, n - image size,

$U(x, y)$ - unit step function,

\oplus - Exclusive or operator

The smaller LOE value is, better it preserve lightness order.

3.7.2 Structure Similarity

Structure Similarity(SSIM) [34] Index is a method used for predicting the perceived quality of similarity between an input image and enhanced result. The range for SSIM is between 0 to 1 with 1 and 0 representing full or no similarity respectively. Higher SSIM value represents better enhanced image.

3.7.3 Naturalness Image Quality Evaluator

Naturalness Image Quality Evaluator(NIQE) [35] calculates no-reference image quality score for an input image using successful space domain Natural Scene Statistic(NSS) model. A smaller score indicates better quality.

3.7.4 No reference Free Energy based Robust Metric

No reference Free Energy based Robust Metric(NFERM) [36] extracts details using classical human visual system and free energy based brain theory to measure degradation in the input image. Lower NFERM means enhanced images are nearer to natural images and are less distorted.

Chapter 4

Results and Analysis

The algorithm proposed has been found promising in image enhancement of sample input noisy, hazy and noiseless images. Experimental results are evaluated with modern image enhancement techniques of Hazy images such as Dark Channel Prior(DCP) [10], No-Black-Pixel Constraint combined with Planar Assumption(NBPCPA) [37], Multi-Scale Convolution Neural Networks(MSCNN) [38], Fast Guided Filter(FGF) [39]. For noisy images, comparison is made with state of the art techniques such as Histogram Equalization, Single scale Retinex [19], and modern techniques such as Contrast-dependent saturation adjustment(CDSA) [40] and Image Enhancement via Illumination Map Estimation(LIME) [21]. Noiseless image comparison is based on state of the art techniques such as Multi-Scale Retinex(MSR) [41] and new techniques such as LIME, CDSA, Naturalness preserved enhancement algorithm(NPEA) [23]. The Parameters of proposed algorithm is provided in the preceding section and algorithms used for comparison are based on the concerned algorithm parameters specified by respective authors. The Data set of input images is taken from various resources. The low light Hazy, Noisy, High Quality images are taken from [42], [24], [14], Caltech data set, Aero-India 2019 web page, Shutterstock website and Internet.

4.1 Qualitative Interpretation

4.1.1 Hazy Image Enhancement

The performance evaluation of enhanced image is based on human judgment and estimation. A total of 29 hazy images are taken for experimental results out of which some are presented here.

Towers



(a) *Original*



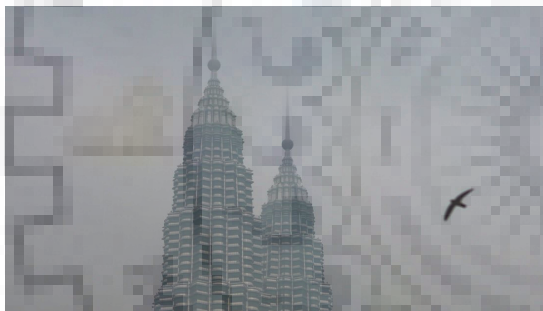
(b) *DCP*



(c) *NBPCPA*



(d) *MSCNN*



(e) *FGF*



(f) *Proposed*

Fig. 4.1. Comparison of Hazy Image Enhancement by various methods

This image is selected as it contains only two tower tops in a hazy background with a bird. The details expected in the enhanced image are clear tower tops with reduced haze and no additional artifacts. The image enhanced by DCP and NBPCPA contains multiple colors and a black patch of noise respectively. FGF enhanced image is still hazy whereas, MSCNN gives a sharper image which exhibits the floor details clearly. The edges of floors in the proposed technique are clearer and sharper with reduced haze than any other technique.

Building and Car



(a) *Original*



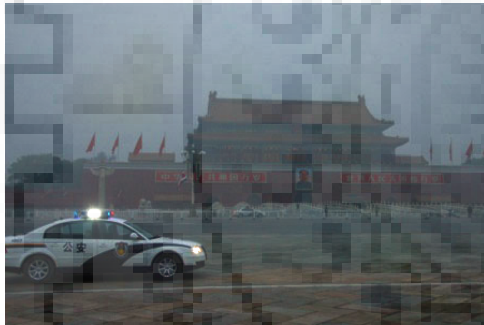
(b) *DCP*



(c) *NBPCPA*



(d) *MSCNN*



(e) *FGF*



(f) *Proposed*

Fig. 4.2. Comparison of Hazy Image Enhancement by various methods

This is an image of a car parked in front of the building. The reason for selecting this image is to observe the details on the car and text written on the building in the hazy environment. Experimental results of DCP and NBPCPA give a darker image which has deteriorated the text on the building. Also, the details on the car, like symbols, are not clearly visible in NBPCPA. The outcome of MSCNN and FGF is improved haze removal in comparison with the previous two techniques, but enhanced images are still dark. The proposed technique gives a clearer and sharper picture in which text on the building and symbols on the car are visible clearly.

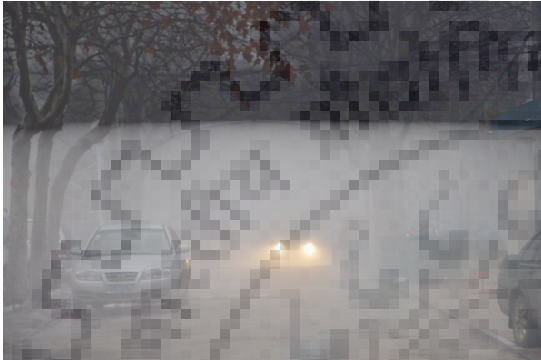
Parked Car



(a) *Original*



(b) *DCP*



(c) *NBPCPA*



(d) *MSCNN*



(e) *FGF*



(f) *Proposed*

Fig. 4.3. Comparison of Hazy Image Enhancement by various methods

The reason for selecting this hazy image is due to availability of multiple items such as car, garbage bins, lights of car, people near the back car, tree leaves, wheel of the car in corner. The image enhanced by both FGF and DCP are darker in comparison to the hazy image even though haze is reduced. The bin box and people are visible in DCP image but not in FGF image. The car light are sprayed and details of car wheel is not visible in case of DCP. The result of NBPCPA is similar to hazy input image with black strip on top. In MSCNN image, car light is not sprayed and the details on the car wheel are protected. But, haze content is similar to the original image with people near the car are not visible. The proposed method gives a clearer image which preserves the details better than other techniques except the details on car wheel which is hidden.

Tree



(a) *Original*



(b) *DCP*



(c) *NBPCPA*



(d) *MSCNN*



(e) *FGF*



(f) *Proposed*

Fig. 4.4. Comparison of Hazy Image Enhancement by various methods

This image contains a single tree with small stones on the surface. This image is selected to check the performance on minimal details in input image of various techniques. DCP and NBPCPA both gives a degraded enhanced image. Results of MSCNN and FGF are similar in which haze is properly removed and surface stones are enhanced well. The proposed method enhances both the tree and stone by removal of haze but image of tree is bit darker.

Mean Opinion Score for Hazy Images

The Mean Opinion Score was calculated for a set of 4 images with 18 members. The image were presented to the members without specifying the method used in a random order. The results of Mean Opinion Score is presented in table 4.1 below:

Method Image	DCP	NBPCPA	MSCNN	FGF	Proposed
Towers	2	1.44	3.28	3.56	4.06
Building and Car	2.56	2.67	2.5	3.44	4.56
Parked car	2.39	1.83	2.94	2.28	3.55
Tree	2	2.28	2.72	3.61	3.55

Table 4.1: Mean Opinion Score for Hazy images enhanced by various methods

4.1.2 Noisy Image Enhancement

Helicopter on Tarmac

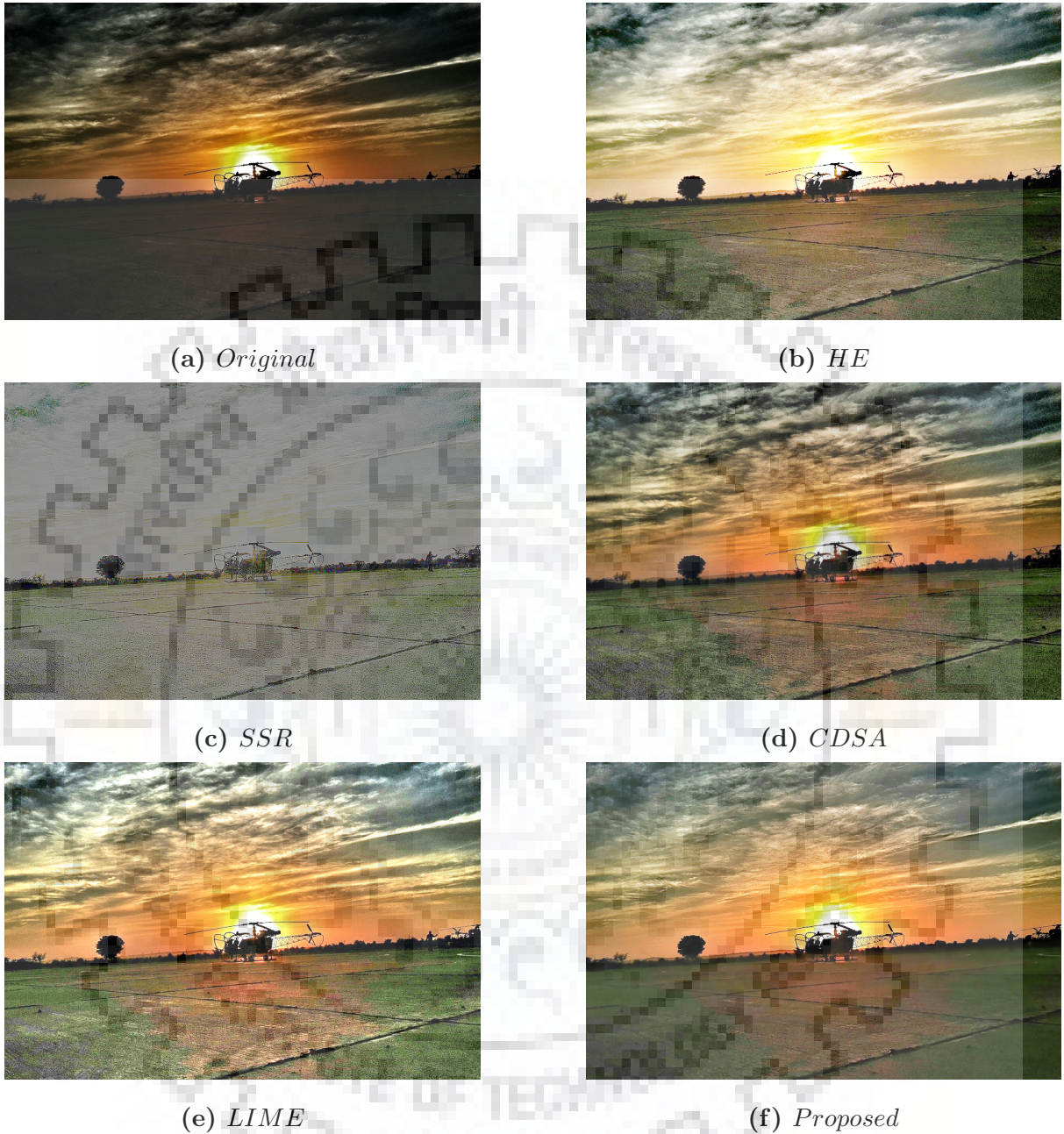


Fig. 4.5. Comparison of Noisy Image Enhancement by various methods

This is a helicopter image standing on tarmac. The image is selected to see the noise removal from the tarmac and preservation of naturalness in the enhanced image. In HE result, even though noise on tarmac is reduced but naturalness of cloud is not preserved. In SSR, the overall image quality is degraded since it does not consider illumination component in image enhancement. The results provided by LIME and CDSA are well enhanced but tarmac is grainy. The proposed method image doesn't contain any grains on the tarmac and overall image naturalness is preserved.

Birds



(a) *Original*



(b) *HE*



(c) *SSR*



(d) *CDSA*



(e) *LIME*



(f) *Proposed*

Fig. 4.6. Comparison of Noisy Image Enhancement by various methods

This image is taken for evaluation as it contains only tree and bird. There is no sky, cloud or ground effect on the image quality. The result by HE is an over-enhanced image in which details of bird and tree leaves are hidden. The image quality is degraded by SSR. The result of LIME is better than CDSA which gives a dark saturated bird even though details of tree are well enhanced. The results of the proposed method are similar to LIME in case of bird with reduced noise but naturalness of tree is well preserved w.r.t. LIME which gives over-enhanced tree.

Fountain

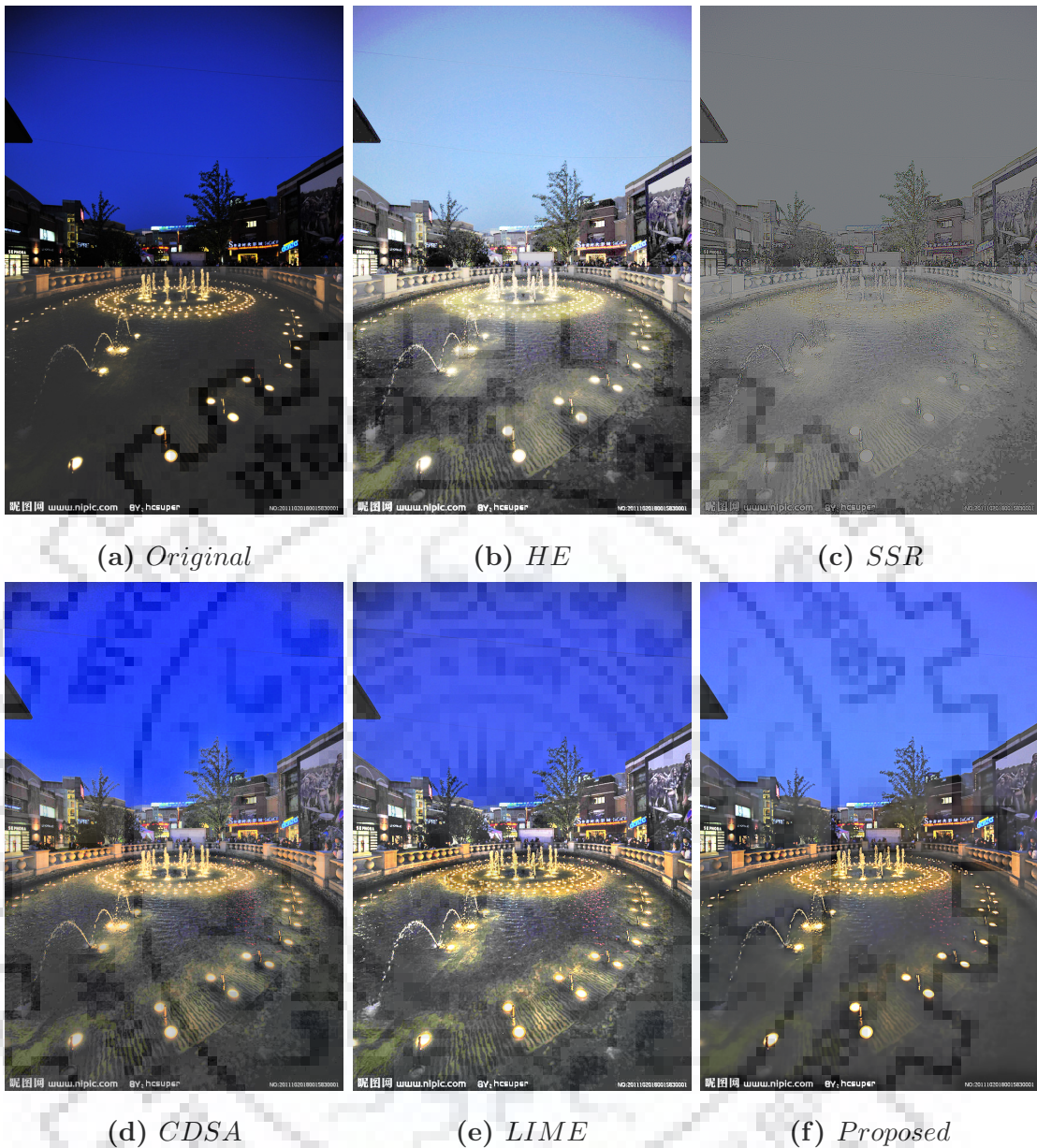


Fig. 4.7. Comparison of Noisy Image Enhancement by various methods

This is a noisy image of a fountain between buildings. The image is selected due to lot of details present in the image. HE enhances the image well but sky color is faded and fountain details are noisy. SSR image is very much degraded in comparison to HE. LIME and CDSA gives a well enhanced image but fountain details are very noisy. The proposed method preserves the details well with reduced noise in comparison to other methods. It loses out on the details of thin wire in top which is visible in case of LIME. This loss of small detail can be ignored in respect of the amount of noise removed.

Flowerpot

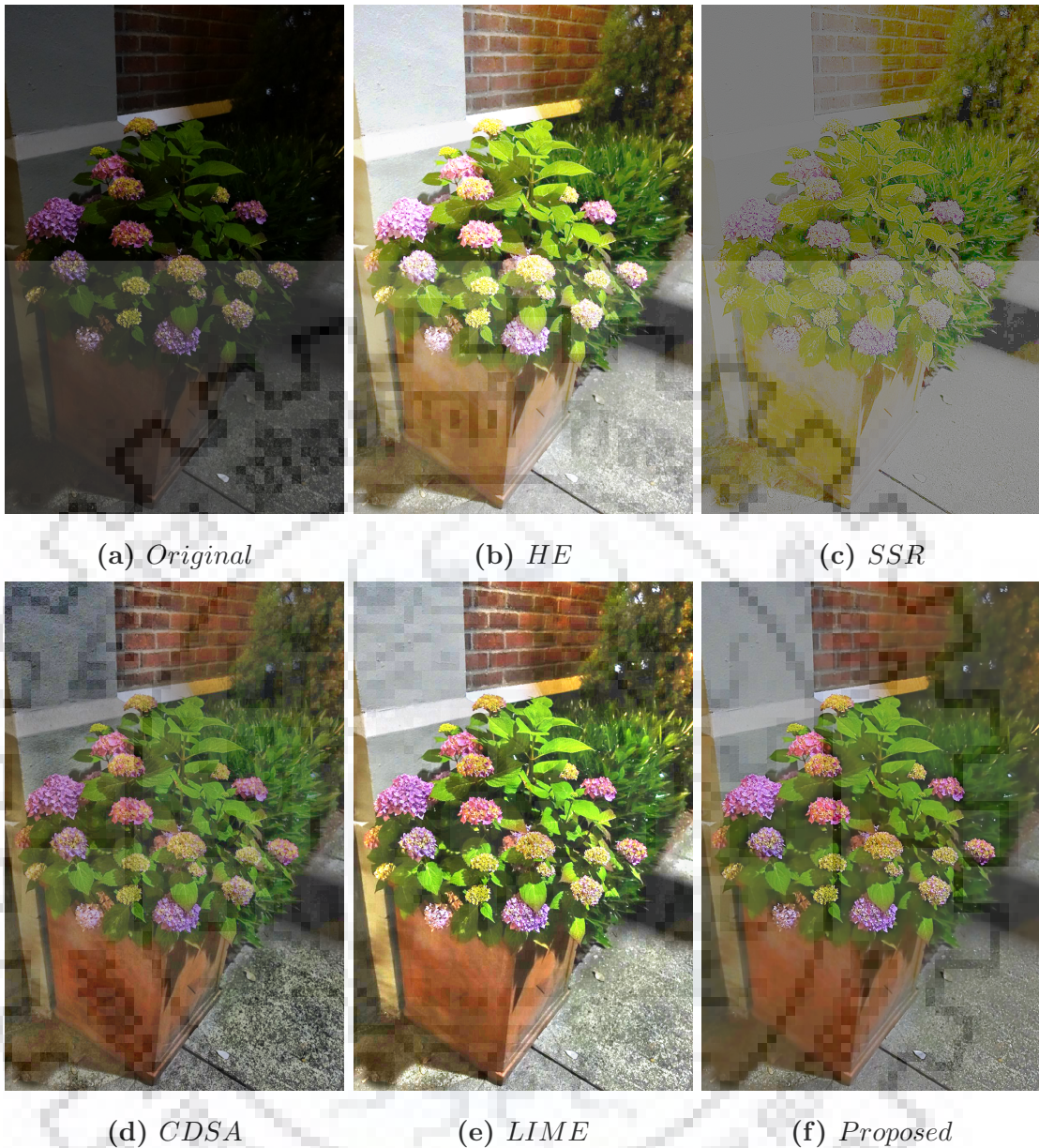


Fig. 4.8. Comparison of Noisy Image Enhancement by various methods

The reason for selecting this image is because it contains lot of details in a small area. Noise is reduced by HE but the color of flowers and flowerpot are faded. In case of SSR image is completely faded and does not look natural. The result of LIME is slightly over enhanced with noise visible below the flowerpot on the surface. CDSA enhanced image looks more natural but surface near pot is more noisy. The proposed method image is natural and less noisy in comparison to any other method.

Mean Opinion Score for Noisy Images

The Mean Opinion Score was calculated for a set of 4 images with 18 members. The image were presented to the members without specifying the method used. The results of Mean Opinion Score is presented in table 4.2 below:

Method Image	HE	SSR	CDSA	LIME	Proposed
H/C on Tarmac	2.72	1.56	3.56	3.28	3.67
Birds	2.39	1.44	2.61	4.27	4.38
Fountain	2.83	2.09	4	3.67	4.11
Flowerpot	4.05	1.33	3.22	4.39	4

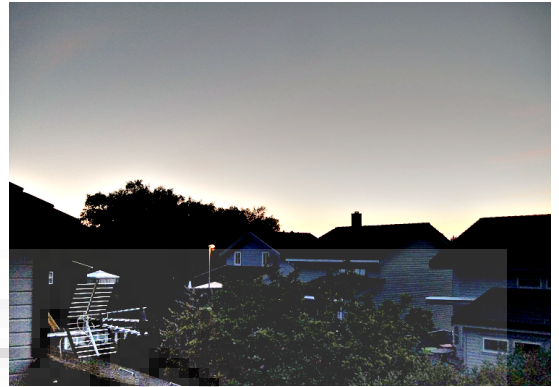
Table 4.2: Mean Opinion Score for Noisy images Enhanced by various methods

4.1.3 Noiseless Image Enhancement

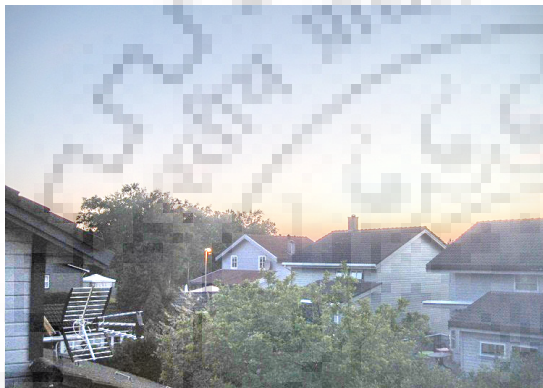
Roofs



(a) *Original*



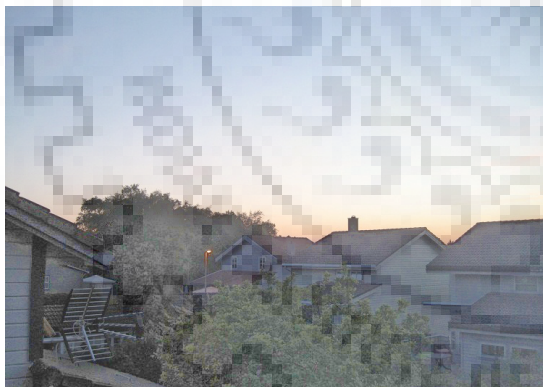
(b) *MSR*



(c) *LIME*



(d) *CDSA*



(e) *NPEA*



(f) *Proposed*

Fig. 4.9. Comparison of Noiseless Image Enhancement by various methods

This is an image which contains multiple roofs, trees, an antenna, chimney on one roof and sky in the background. Image is selected for overall enhancement and naturalness preservation with minute details. The MSR enhanced image is oversaturated due to which details are suppressed. The CDSA and NPEA enhances the image well but cloud color doesn't look natural and chimney color partitions are not visible in CDSA whereas, in case of NPEA tree in background and chimney details are not clear. The LIME results in an over enhanced image(brightness of the antenna is more pronounced). The proposed

method enhances the image well and the details of chimney and naturalness of the sky is well preserved.

Old Building



(a) *Original*



(b) *MSR*



(c) *LIME*



(d) *CDSA*



(e) *NPEA*



(f) *Proposed*

Fig. 4.10. Comparison of Noiseless Image Enhancement by various methods

In this image of an old building with grass and clouds, the MSR results in a saturated image, whereas LIME image is over-enhanced. In case of CDSA, the details of clouds on the corner are bit darker even though other details are well preserved. NPEA and proposed method gives better enhanced image but details of the building are more pronounced in the proposed method.

Lamp and Shrub



(a) *Original*



(b) *MSR*



(c) *LIME*



(d) *CDSA*



(e) *NPEA*



(f) *Proposed*

Fig. 4.11. Comparison of Noiseless Image Enhancement by various methods

In the present image, preservation of lamp and shrub naturalness among clutter of details like buildings, trees, sky etc is to be observed. In case of MSR, image is oversaturated. In case of LIME and NPEA the details of shrub is subdued. The CDSA and proposed method gives well enhanced image. Details of lamp are more clear in proposed method than CDSA.

Trees



(a) *Original*



(b) *MSR*



(c) *LIME*



(d) *CDSA*



(e) *NPEA*



(f) *Proposed*

Fig. 4.12. Comparison of Noiseless Image Enhancement by various methods

This image is selected for naturalness preservation during enhancement. The image enhanced by MSR is saturated as can be observed by trees and sky whereas LIME results in a over enhanced image. The NPEA enhanced image contains noisy patches on the tree and shadow. There is more clarity in CDSA image whereas naturalness is well preserved in the proposed image.

Mean Opinion Score for Noiseless Images

The Mean Opinion Score was calculated for a set of 4 images with 18 members. The image were presented to the members without specifying the method used. The results of Mean Opinion Score is presented in table 4.3 below:

Method Image	MSR	LIME	CDSA	NPEA	Proposed
Roofs	1.78	3.72	3.67	3.28	3.78
Old Build- ing	1.72	3.78	4.06	4.22	3.83
Lamp and Shrub	3.11	3.22	4.11	2.72	3.67
Trees	2.06	3.44	4.17	2.72	4.33

Table 4.3: Mean Opinion Score for images Enhanced by various methods

4.2 Qualitative Interpretation by Edge Detection for Noisy Image

Helicopter on Tarmac

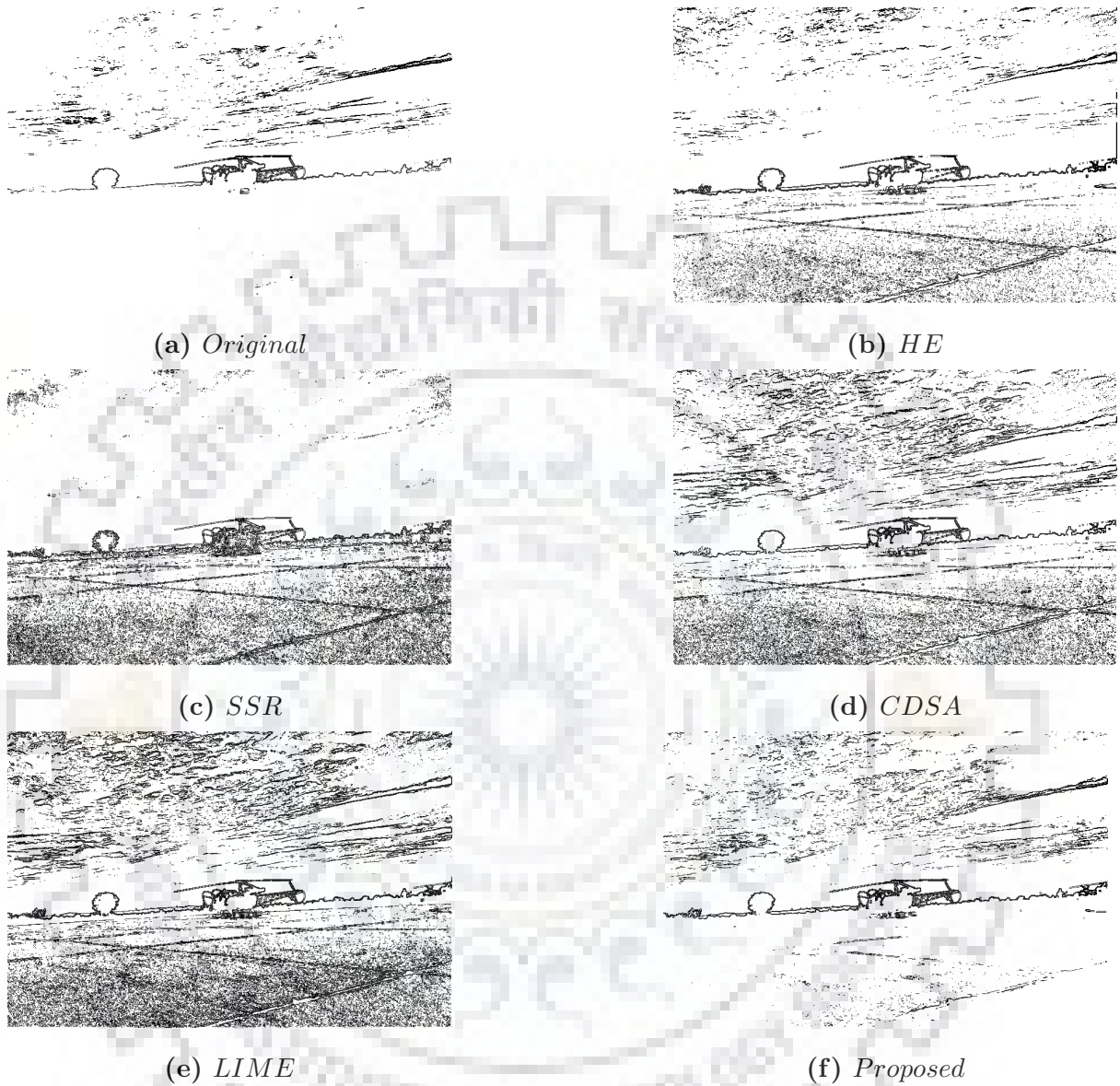


Fig. 4.13. Comparison of Sobel Edges in Noisy Image Enhanced by various methods. In the image of fig 4.13, sobel edge detector is applied on the original and enhanced image obtained by various methods. A threshold of 150 is applied while using the sobel edge detector. In the original image, the noise is minimum but details of ground edges and some details pertaining to the helicopter landing gear are lost. In SSR, CDSA and LIME the content of noise in the image is high which is visible from the black grains on the ground. HE enhanced image edges are more clearly visible with less noise as compared to SSR, CDSA and LIME. In, proposed method, ground noise is low and helicopter details are well preserved. There is a little loss of details on the ground which can be ignored since the amount of noise is greatly reduced.

4.3 Quantitative Measurement

4.3.1 Structure Similarity

The SSIM values of different methods for hazy images is being plotted in Fig. 4.14. Higher SSIM value represents better preservation of details in the enhanced image w.r.t. input image. It can be observed from the plot that result of proposed method is better or similar to other techniques for the test images.

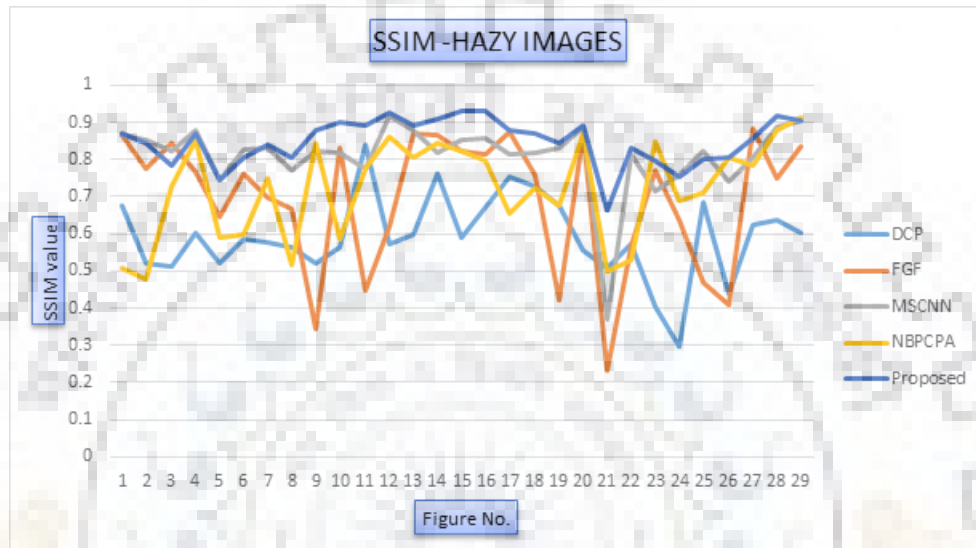


Fig. 4.14. SSIM for Hazy Images

The SSIM values for different methods in case of noisy images is being plotted in Fig. 4.15. It can be observed from the plot that result of proposed method is better than other techniques in preservation of details.

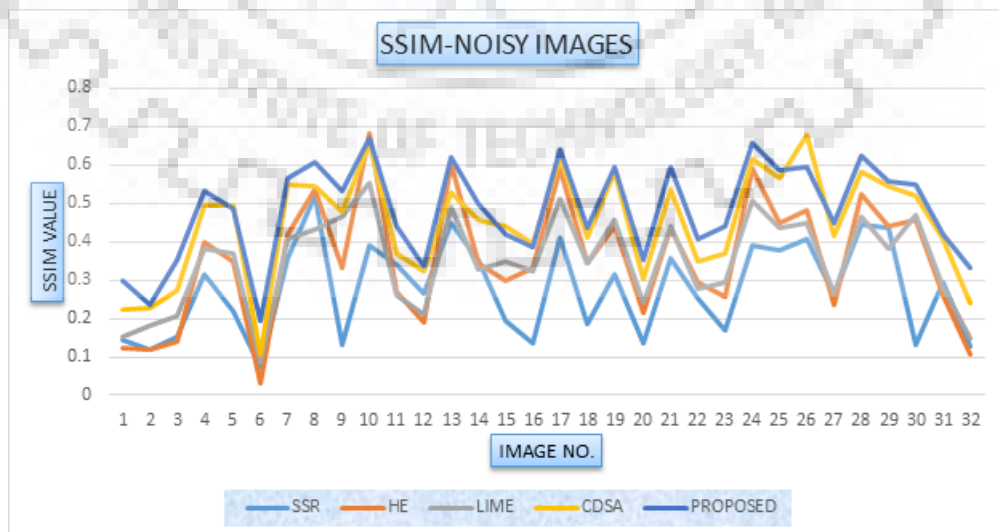


Fig. 4.15. SSIM for Noisy Images

The SSIM values for noiseless images is being plotted in Fig. 4.16. It can be observed from the plot that average SSIM value result of proposed technique is better than other techniques in preservation of details. NPEA results are almost similar to proposed method.

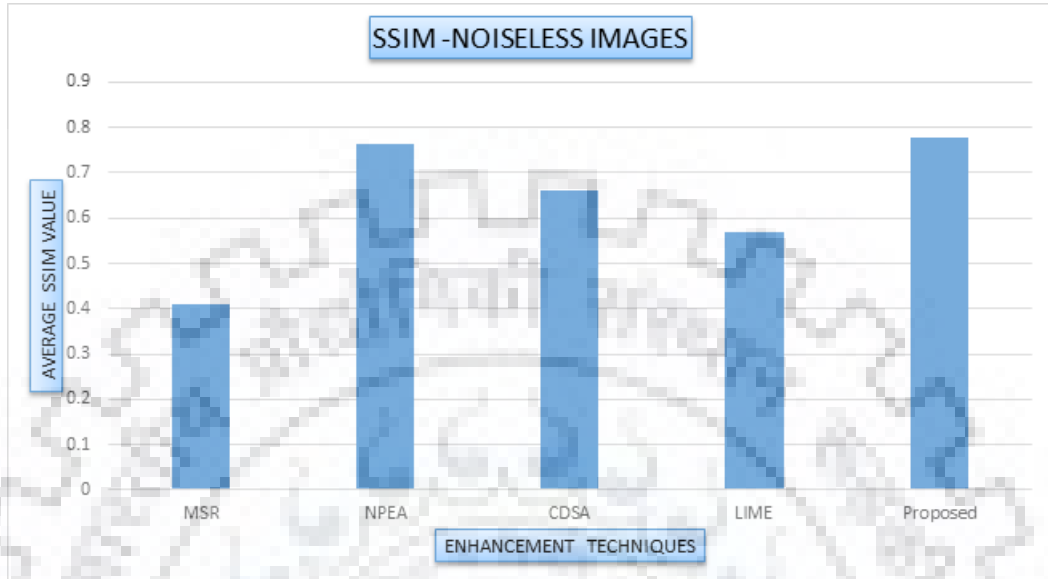


Fig. 4.16. Average SSIM for Noiseless Images

4.3.2 Lightness Order Error

The LOE values for noiseless images is being plotted in Fig. 4.17. According to the definition, higher LOE value means poorer lightness equality preservation. As we can see, NPEA and proposed method both are good in preserving the lightness inequality.

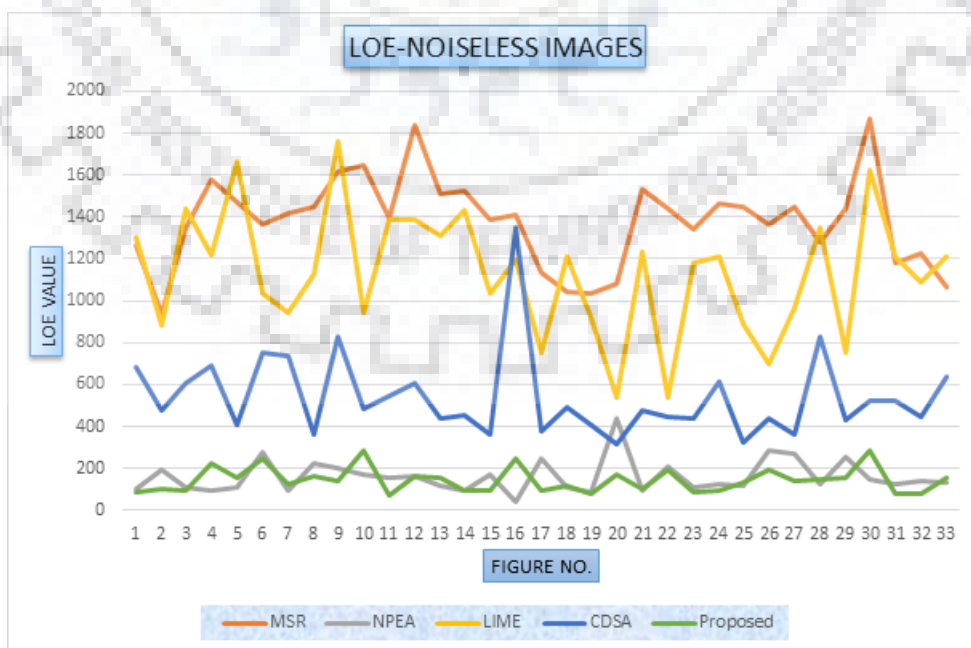


Fig. 4.17. LOE for Noiseless Images

4.3.3 No reference Free Energy based Robust Metric

The NFERM result for noiseless images is being plotted in Fig. 4.18. According to the definition, lower NFERM value means better features extraction in order to evaluate the distortion of input image and enhanced image. The plots shows that, result of proposed technique outperforms other methods in most of the cases.

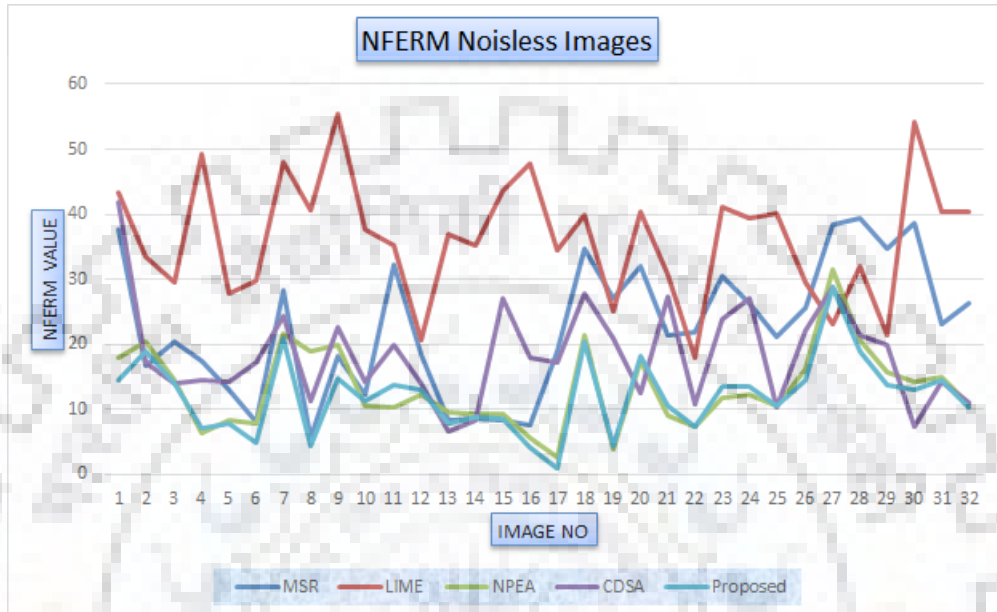


Fig. 4.18. NFERM for Noiseless Images

4.3.4 Naturalness Image Quality Evaluator

The average value for NIQE metric are presented for evaluation of different methods in Fig. 4.19. A lower value of the parameter present better naturalness preservation of the enhanced image w.r.t. input image. It can be observed that the results of proposed technique are better than other methods.

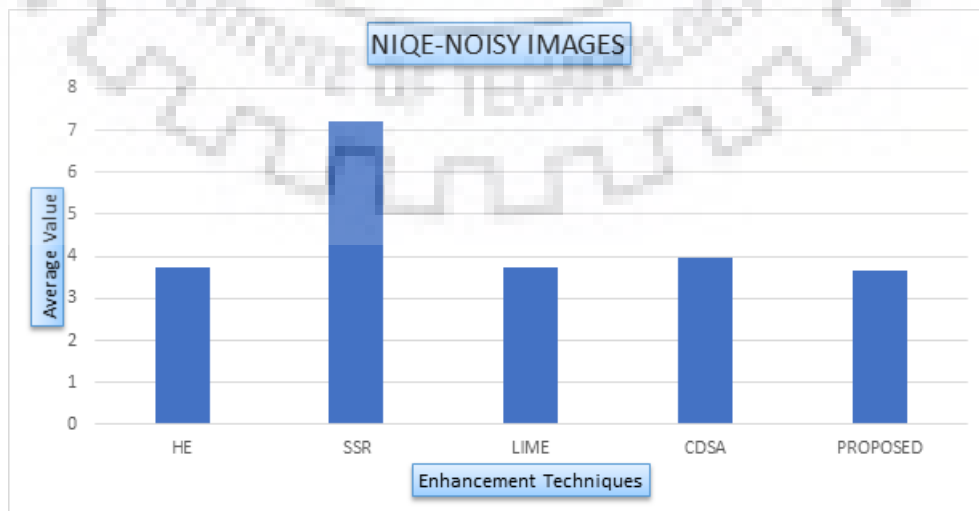


Fig. 4.19. NIQE for Noisy Images

Chapter 5

Conclusion and Future Work

In this report, an integrated approach for classification and enhancement of an input low light hazy, noisy and noiseless images is being carried out. The classification of an image into hazy and non hazy is being developed around a threshold value of 1.16. Success rate of 95% is achieved in hazy image classification. Further classification of images into noisy and noiseless is carried out using linear SVM classifier. Classification accuracy for noisy images is around 85% . Once images are classified, enhancement is being carried out. Hazy image enhancement is carried out using Multilayer Perceptron of Artificial Neural Network. Retinex based methods utilizing image decomposition into reflectance and illumination component through iterative approach and Multi-Layer lightness statistics is used for enhancement of noisy and noiseless images respectively. A comparative analysis of various method based on Qualitative and Quantitative metrics such as MOS, SSIM, NIQE, NFERM is being carried out.

It can be concluded that the image classification into hazy and noisy using visibility Parameter and Support Vector Machine Classifier is novel and works well with wide variety of images. Further enhancement of images using integrated proposed approach has performed better or similar than other algorithms for enhancement of noisy and hazy images.

In future, improvements to SVM classifier will be made to increase the success rate of classification. Further, study will be made for enhancement of dusty low light images and identification of small objects in a dusty environment. The study of noise and dust removal on a single image will be extended to real time videos for identification of target hit point of bullets and rockets towards Circular Error Probability calculation.

Bibliography

- [1] R. C. Gonzalez, R. E. Woods, S. L. Eddins *et al.*, *Digital image processing using MATLAB*. Pearson-Prentice-Hall Upper Saddle River, New Jersey, 2004, vol. 624.
- [2] R. C. Gonzalez and R. E. Woods, “Image processing,” *Digital image processing*, vol. 2, 2007.
- [3] R. K. Thakur and C. Saravanan, “Classification of color hazy images,” in *2016 International Conference on Electrical, Electronics, and Optimization Techniques (ICEEOT)*. IEEE, 2016, pp. 2159–2163.
- [4] Y. Y. Schechner, S. G. Narasimhan, and S. K. Nayar, “Instant dehazing of images using polarization,” in *CVPR (1)*, 2001, pp. 325–332.
- [5] S. Fang, X. Xia, X. Huo, and C. Chen, “Image dehazing using polarization effects of objects and airlight,” *Optics express*, vol. 22, no. 16, pp. 19 523–19 537, 2014.
- [6] J. Kopf, B. Neubert, B. Chen, M. Cohen, D. Cohen-Or, O. Deussen, M. Uyttendaele, and D. Lischinski, *Deep photo: Model-based photograph enhancement and viewing*. ACM, 2008, vol. 27, no. 5.
- [7] C. Chengtao, Z. Qiuyu, and L. Yanhua, “A survey of image dehazing approaches,” in *The 27th Chinese Control and Decision Conference (2015 CCDC)*. IEEE, 2015, pp. 3964–3969.
- [8] M. M. Singh, “A survey paper on single image dehazing,” *International Journal on Recent and Innovation Trends in Computing and Communication*, vol. 3, no. 2, pp. 085–088, 2015.
- [9] J.-P. Tarel and N. Hautiere, “Fast visibility restoration from a single color or gray level image,” in *2009 IEEE 12th International Conference on Computer Vision*. IEEE, 2009, pp. 2201–2208.

- [10] K. He, J. Sun, and X. Tang, "Single image haze removal using dark channel prior," *IEEE transactions on pattern analysis and machine intelligence*, vol. 33, no. 12, pp. 2341–2353, 2011.
- [11] J. Pang, O. C. Au, and Z. Guo, "Improved single image dehazing using guided filter," *Proc. APSIPA ASC*, pp. 1–4, 2011.
- [12] M. W. Gardner and S. Dorling, "Artificial neural networks (the multilayer perceptron)—a review of applications in the atmospheric sciences," *Atmospheric environment*, vol. 32, no. 14-15, pp. 2627–2636, 1998.
- [13] D. Kriesel, *A brief introduction to neural networks*, 2005, vol. 1(1).
- [14] S. Salazar-Colores, I. Cruz-Aceves, and J.-M. Ramos-Arreguin, "Single image dehazing using a multilayer perceptron," *Journal of Electronic Imaging*, vol. 27, no. 4, p. 043022, 2018.
- [15] N. Cristianini, J. Shawe-Taylor *et al.*, *An introduction to support vector machines and other kernel-based learning methods*. Cambridge university press, 2000.
- [16] S. M. Pizer, R. E. Johnston, J. P. Ericksen, B. C. Yankaskas, and K. E. Muller, "Contrast-limited adaptive histogram equalization: speed and effectiveness," in *[1990] Proceedings of the First Conference on Visualization in Biomedical Computing*. IEEE, 1990, pp. 337–345.
- [17] M. Abdullah-Al-Wadud, M. H. Kabir, M. A. A. Dewan, and O. Chae, "A dynamic histogram equalization for image contrast enhancement," *IEEE Transactions on Consumer Electronics*, vol. 53, no. 2, pp. 593–600, 2007.
- [18] E. H. Land, "The retinex theory of color vision," *Scientific American*, vol. 237, no. 6, pp. 108–129, 1977.
- [19] G. Hines, Z.-u. Rahman, D. Jobson, and G. Woodell, "Single-scale retinex using digital signal processors," 2005.
- [20] Z. Liang, W. Liu, and R. Yao, "Contrast enhancement by nonlinear diffusion filtering," *IEEE Transactions on Image Processing*, vol. 25, no. 2, pp. 673–686, 2016.
- [21] X. Guo, Y. Li, and H. Ling, "Lime: Low-light image enhancement via illumination map estimation." *IEEE Trans. Image Processing*, vol. 26, no. 2, pp. 982–993, 2017.

- [22] X. Fu, Y. Liao, D. Zeng, Y. Huang, X.-P. Zhang, and X. Ding, “A probabilistic method for image enhancement with simultaneous illumination and reflectance estimation,” *IEEE Transactions on Image Processing*, vol. 24, no. 12, pp. 4965–4977, 2015.
- [23] S. Wang, J. Zheng, H.-M. Hu, and B. Li, “Naturalness preserved enhancement algorithm for non-uniform illumination images,” *IEEE Transactions on Image Processing*, vol. 22, no. 9, pp. 3538–3548, 2013.
- [24] S. Wang and G. Luo, “Naturalness preserved image enhancement using a priori multi-layer lightness statistics,” *IEEE transactions on image processing: a publication of the IEEE Signal Processing Society*, vol. 27, no. 2, pp. 938–948, 2018.
- [25] X. Zhang, P. Shen, L. Luo, L. Zhang, and J. Song, “Enhancement and noise reduction of very low light level images,” in *Proceedings of the 21st International Conference on Pattern Recognition (ICPR2012)*. Ieee, 2012, pp. 2034–2037.
- [26] L. Li, R. Wang, W. Wang, and W. Gao, “A low-light image enhancement method for both denoising and contrast enlarging,” in *2015 IEEE International Conference on Image Processing (ICIP)*. IEEE, 2015, pp. 3730–3734.
- [27] K. Dabov, A. Foi, and K. Egiazarian, “Video denoising by sparse 3d transform-domain collaborative filtering,” in *2007 15th European Signal Processing Conference*. IEEE, 2007, pp. 145–149.
- [28] M. Li, J. Liu, W. Yang, X. Sun, and Z. Guo, “Structure-revealing low-light image enhancement via robust retinex model,” *IEEE Transactions on Image Processing*, vol. 27, no. 6, pp. 2828–2841, 2018.
- [29] R. M. Haralick, K. Shanmugam *et al.*, “Textural features for image classification,” *IEEE Transactions on systems, man, and cybernetics*, no. 6, pp. 610–621, 1973.
- [30] A. Levin, D. Lischinski, and Y. Weiss, “A closed-form solution to natural image matting,” *IEEE transactions on pattern analysis and machine intelligence*, vol. 30, no. 2, pp. 228–242, 2008.
- [31] C.-C. Yang, “Image enhancement by modified contrast-stretching manipulation,” *Optics & Laser Technology*, vol. 38, no. 3, pp. 196–201, 2006.

- [32] B. Li, S. Wang, J. Zheng, and L. Zheng, "Single image haze removal using content-adaptive dark channel and post enhancement," *IET Computer Vision*, vol. 8, no. 2, pp. 131–140, 2014.
- [33] "Mean Opinion Score," https://en.wikipedia.org/wiki/Mean_opinion_score, accessed: 2018-11-17.
- [34] Z. Wang, A. C. Bovik, H. R. Sheikh, E. P. Simoncelli *et al.*, "Image quality assessment: from error visibility to structural similarity," *IEEE transactions on image processing*, vol. 13, no. 4, pp. 600–612, 2004.
- [35] A. Mittal, R. Soundararajan, and A. C. Bovik, "Making a "completely blind" image quality analyzer," *IEEE Signal Processing Letters*, vol. 20, no. 3, pp. 209–212, 2013.
- [36] K. Gu, G. Zhai, X. Yang, and W. Zhang, "Using free energy principle for blind image quality assessment," *IEEE Transactions on Multimedia*, vol. 17, no. 1, pp. 50–63, 2015.
- [37] J.-P. Tarel, N. Hautiere, L. Caraffa, A. Cord, H. Halmaoui, and D. Gruyer, "Vision enhancement in homogeneous and heterogeneous fog," *IEEE Intelligent Transportation Systems Magazine*, vol. 4, no. 2, pp. 6–20, 2012.
- [38] W. Ren, S. Liu, H. Zhang, J. Pan, X. Cao, and M.-H. Yang, "Single image dehazing via multi-scale convolutional neural networks," in *European conference on computer vision*. Springer, 2016, pp. 154–169.
- [39] K. He, J. Sun, and X. Tang, "Guided image filtering," *IEEE transactions on pattern analysis and machine intelligence*, vol. 35, no. 6, pp. 1397–1409, 2012.
- [40] S. Wang, W. Cho, J. Jang, M. A. Abidi, and J. Paik, "Contrast-dependent saturation adjustment for outdoor image enhancement," *JOSA A*, vol. 34, no. 1, pp. 7–17, 2017.
- [41] D. J. Jobson, Z.-u. Rahman, and G. A. Woodell, "A multiscale retinex for bridging the gap between color images and the human observation of scenes," *IEEE Transactions on Image processing*, vol. 6, no. 7, pp. 965–976, 1997.
- [42] S. Wang, Y. Tian, T. Pu, and P. Wang, "A hazy image database with analysis of the frequency magnitude," 09 2017.